NRL Report 6673

Power Spectrum Estimates of Sampled Pseudo-Random Sequences

CALDWELL MCCOY, JR.

Signal Processing Branch
Acoustics Division

December 29, 1967

NAVAL RESEARCH LABORATORY
Washington, D.C.

This document has been approved for public release and sale; its distribution is unlimited.

This report is a thesis submitted to The George Washington University in partial fulfillment for the degree of Master of Science to be conferred February 22, 1968. The manuscript was submitted for an NRL Report, November 28, 1967.

ABSTRACT

This report concerns power spectrum estimates of sampled pseudo-random signals, and shows that for these signals the spectral power is more relevant than, say, the autocorrelation function. The power spectrum estimates considered here assume stationarity and zero means.

The signal under investigation is a pseudo-random noise signal obtained from maximal length sequences. Pseudo-random signals are popular because (a) they can be fashioned with relative ease from linear shift registers, (b) their deterministic waveforms have uniform power throughout their bandwidths, and (c) their autocorrelations are approximately zero outside a narrow peak at zero tau.

This study is concerned with some applied methods and results of these applications to bandlimited signals that have been corrupted by additive-noise, multiple-path, and Doppler effects and that have been processed digitally to obtain correlations and power spectra. The object was to observe the effects on the power spectrum estimates due to these perturbations. The analysis was performed exclusively on filtered maximal length pseudo-random sequences. These filtered sequences were tailored to a bandwidth and sample size to yield optimal results for a given computer memory capability.

PROBLEM STATUS

This is an interim report on the problem; work is continuing.

AUTHORIZATION

NRL Problem S01-06
Project RF 101-03-44-4054

ACKNOWLEDGMENTS

I am indebted to Professor Jhong S. Lee of the George Washington University under whose guidance and direction this work was performed.

This research was performed at the U.S. Naval Research Laboratory. I greatly appreciate the encouragement received from H. L. Peterson, Acting Head, Signal Processing Branch, Acoustics Division. Thanks are also due to my associates, D. A. Swick for his critical discussions and G. G. Nacht and C. E. Balfourd for their technical assistance, and to the Technical Information Division for their assistance in preparation of this thesis.

TABLE OF CONTENTS

	Page
ACKNOWLEDGMENTS	ii
INTRODUCTION	1
PSEUDO-RANDOM SEQUENCES	2
CORRELATION	7
POWER SPECTRUM	10
Measurement of Power Spectrum	11
Output Power Versus Frequency	12
BANDWIDTHS	14
SAMPLING ANALYSIS	16
FILTERING	17
PN SIGNATURE	18
COMPUTER PROGRAM	19
EXPERIMENTAL RESULTS	22
Pseudo-Noise Signature	22
Additive Noise Effect	31
Multiple-Path Effect	44
Doppler Effect	53
CONCLUSIONS	64
REFERENCES	65
APPENDIX A – PROPERTIES OF PSEUDO-RANDOM SEQUENCES	67
APPENDIX B – MATHEMATICAL CONCEPTS	71
APPENDIX C – DEFINITIONS OF STATISTICAL TERMS	79

LIST OF FIGURES

Figure		Page
1	Three-stage shift register with mod-2 feedback	3
2	Truth table for mod-2 addition	3
3	Table of taps for various shift register lengths to generate corresponding maximal length sequences	6
4	Autocorrelation function of a maximal length sequence	9
5	Power spectrum of wideband pseudo-random noise	13
6	Digital recording system with eight channels of multiplexing	20
7	Digital recording of PN at various shift rates and sampling rates	24
8	Power spectrum estimates and autocorrelation of bandlimited PN (case 1 of Table 1: BW = 150-250 Hz; Z = 1023 bits) (a) power spectrum estimates (b) autocorrelation	27
9	Power spectrum estimates and autocorrelation of bandlimited PN (case 16 of Table 1: BW = 350 - 450 Hz; Z = 1023 bits) (a) power. spectrum estimates (b) autocorrelation	28
10	Power spectrum estimates and autocorrelation of bandlimited PN (case 2 of Table 1: BW = 150-250 Hz; Z = 2047 bits) (a) power spectrum (b) autocorrelation	29
11	Power spectrum estimates and autocorrelation of bandlimited PN (case 3 of Table 1: BW = 150-250 Hz; Z = 4095 bits) (a) power spectrum (b) autocorrelation	30
12	Digital recording of PN with additive noise	33
13	Spectrum of wideband thermal noise (case 1 of Table 2) (a) spectrum of wideband thermal noise (b) autocorrelation	38
14	Effects of additive wideband thermal noise on the bandlimited PN power spectrum and correlation (case 8 of Table 2: S/N ratio = 0 dB) (a) power spectrum (b) autocorrelation	39
15	Power spectrum and correlations of additive thermal noise and PN (case 10 of Table 2: S/N ratio = –10 dB) (a) power spectrum (b) autocorrelation (c) crosscorrelation of the reference PN signal and case 10	40

LIST OF FIGURES – Continued

Figure		Page
16	Spectrum of narrowband thermal noise (case 15 of Table 2: BW = 150-250 Hz) (a) power spectrum (b) autocorrelation	41
17	Effects of additive thermal noise on PN power spectrum and correlations – both bandlimited (case 22 of Table 2: BW = 150-250 Hz; S/N ratio = 0 dB) (a) power spectrum (b) autocorrelation (c) crosscorrelation of case 16 (reference PN) against case 22	42
18	Effects of additive thermal noise on PN power spectrum and correlations – both bandlimited (case 24 of Table 2: BW = 150-250 Hz; S/N ratio = –10 dB) (a) power spectrum (b) autocorrelation (c) crosscorrelation of the case 16 against case 24	43
19	Multiple-path effects	45
20	Effects of single multipath on PN power spectrum and correlations (case 3 of Table 3: BW = 150-250 Hz; multipath = 5 ms) (a) power spectrum (b) autocorrelation (c) crosscorrelation of the reference PN against case 3	48
21	Effects of single multipath on PN power spectrum and correlations (case 9 of Table 3: BW = 150-450 Hz; multipath = 5 ms) (a) power spectrum (b) autocorrelation (c) crosscorrelation of the reference PN against case 9	49
22	Doppler effect (a) f waves crowded into space $c - v_s$ (b) observer receives waves in space $c + v_o$ each second	54
23	Doppler effects on PN power spectrum and correlations (case 2 of Table 4: BW = 150-250 Hz; Doppler shift = 0.4 Hz) (a) smoothed spectrum (b) unsmoothed spectrum (c) autocorrelation (d) crosscorrelation of the reference PN against case 2	60 & 61
24	Doppler effects on PN power spectrum and correlations (case 6 of Table 4: BW = 150-250 Hz; Doppler shift = 1.8 Hz) (a) smoothed spectrum (b) unsmoothed spectrum (c) autocorrelation (d) crosscorrelation of the reference PN against case 6	62 & 63

LIST OF TABLES

Table		Page
1	Cases recorded for PN sequences of shift register lengths 10, 11, and 12	26
2	Cases recorded for PN sequences with additive noise	37
3	Cases recorded for effects of multipath on PN sequences	45
4	Cases recorded for effects of Doppler on PN sequences	57

INTRODUCTION

Power spectrum density may be the most significant statistical property of a signal. For some special classes of signals, the spectral power may continue to reveal useful information where other statistical measurements fail.

This thesis concerns power spectrum analysis of sampled pseudo-random signals and shows that for these signals the spectral power is more relevant than, say, the autocorrelation function. The power spectrum estimates considered here assume stationarity and zero averages but do not depend upon the Gaussian assumption. It will present the correlations along with the spectral estimates for comparison. As a means for understanding and as a guide for intelligent design, the power spectrum is without peer [1].

Correlation functions are of little use except as a basis for estimating the power spectrum. In most physical systems, power spectra have reasonable shapes, are relatively easily understood, and are directly influenced by the basic variables of the situation.

The signals used throughout this report are maximal length pseudo-random sequences. The thesis will define maximal length sequences, establish their general properties, show how many maximal length sequences can be obtained from a given nth-degree linear shift register, how to select the taps for maximal length sequences, and finally how to express the sequence in the form of a polynomial.

This study is concerned with some applied methods and results of these applications to band-limited signals that have been corrupted by additive-noise, multiple-path, and Doppler effects and have been processed digitally to obtain correlations and power spectra. The object of this analysis is to observe the effects on the power spectrum estimates of these corruptions to the signal, when taken individually. The collective effects of these corruptions are also important but are beyond the scope of this thesis. The analysis is performed exclusively on filtered maximal length pseudo-random sequences. These filtered sequences are tailored to a bandwidth and sample size which yields the most meaningful results for a given computer memory size.

The analysis and data handling are performed by digital techniques rather than analog. It would be most desirable to do everything in real time (on line) entirely on a continuous basis, but such a system is not available for practical use. The digital system will always be an approximation to the true continuous representation but is more reliable than an analog system. The problems of drift, nonlinearity, and bandwidth,

although present in digital systems, do not have the same adverse effects as in an analog system which provides continuous analysis. Even if all the data were handled in a strictly analog system and computed in real time, the final answers would still have to be approximated, whether they were to be typed out or read from a graph or oscilloscope.

Even if all human errors could be omitted in the calculations, there would still remain a number of fundamental sources of difficulty in measuring power spectra. The most basic problem is due to the fact that the actual record lengths are finite rather than infinite in extent; consequently it is not possible to deal with a single frequency but only with a finite band which has greater than zero width. This leads to errors in *resolution* that cannot be surmounted. It is therefore not physically possible to measure power at some exact value of frequency – this would require an infinite time interval. The measurements here are thus power spectrum estimates which yield the power in the neighborhood of the frequency or frequencies of interest.

PSEUDO-RANDOM SEQUENCES

The use of pseudo-random sequences in radar, communications, and ocean acoustic research has gained widespread popularity over the past decade. This popularity of pseudo-random signals can be attributed to the relative ease with which they can be fashioned from sequence generators, to the waveform, which is deterministic with uniform power throughout its bandwidth, and to the autocorrelation function, which is approximately zero outside a narrow peak at zero tau.

A pseudo-random sequence will be defined as a sequence of binary bits (zeros and ones) that appear to be random in their occurrence but which have been produced by a deterministic device such as a linear shift register. This linear shift register will produce a deterministic sequence due to its feedback arrangement, giving a noiselike pseudo-random sequence of zeros and ones rather than a true random sequence [2, 3]. (The term pseudo-random will be abbreviated as PN for pseudo-random noise, and the designation PN sequence will be used interchangeably with PN signal.)

The implementation of a PN sequence will generally be by a linear shift register of length n-bits, employing modulo-2 feedback as shown in Fig. 1. The truth table for modulo-2 addition, Fig. 2, is the same as that for an *exclusive or* operation, an *even parity* generator, or a *half adder*.

The sequences that will be used in this study are called maximal length sequences. their periods will be $2^n - 1$ bits, where n is the number of stages employed in the shift register. If modulo-2 addition is assumed, the sequence of zeros and ones will have the following properties [2].

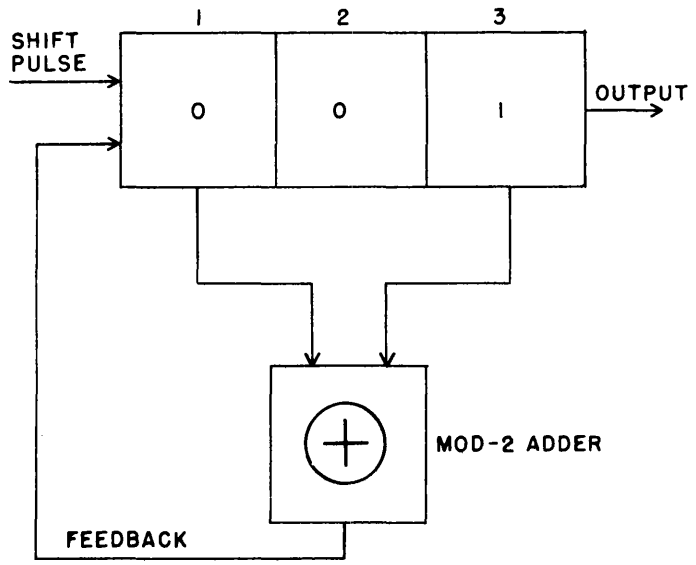

Fig. 1 – Three-stage shift register with mod-2 feedback

x	y	f
0	0	0
0	1	1
1	0	1
1	1	0

$f = x\bar{y} + y\bar{x}$

Fig. 2 – Truth table for mod-2 addition

A. (Balance) – In each period of the sequence the number of ones will be exactly one more than the number of zeros.

B. (Runs) – Among the runs of ones and zeros in each period, one-half of the runs of each kind are of length one, one-fourth are of length two, one-eighth are of length three, etc., until these fractions cease to give meaningful numbers of runs.

C. (Correlation) – If a period of the sequence is compared, term by term, with any nontrivial cyclic shift of itself, the number of agreements differs from the number of disagreements by exactly one.

In properties A and C the wording *exactly one* has been substituted for the usual wording of *at most one*, because this author feels that there is room for possible confusion otherwise.

An **n**-stage linear shift register, commonly referred to as a shift register of degree **n**, can generate a maximum sequence of length $z = 2^n - 1$ bits. Since there are 2^n different **n**-tuple (**n**-digit) binary numbers, 2^n would appear to be the maximum length sequence generated, but a state of all zeros in the shift register is disallowed, since the mod-2 feedback would then yield nothing but zeros. Therefore the maximum output sequence period for a linear shift register of degree **n** is $2^n - 1$.

A given generator can be connected to give maximal or nonmaximal length sequences, but this study will concern itself with the maximal lengths only. It will be instructive at this point for us to examine how the maximal lengths are obtained and how they behave.

Figure 1 will serve as an example for the implementation of our maximal length sequence. This figure shows a three-stage shift register (a register of degree three); it becomes a generator with the employment of feedback. The output is then of greater length than the storage capacity of the shift register. The feedback comes from a mod-2 adder and will always be fed to the first stage of the shift register. The output can be taken from any stage; for convenience we will use the nth stage only.

The number of stages feeding the mod-2 adder must be even to generate a maximal length $z = 2^n - 1$. The proof of this lies in the truth table associated with the mod-2 feedback. In an odd-tap arrangement to the mod-2 adder the all-ones state is denied in addition to the all-zeros state, which is always disallowed. Neither of these states would allow the shift register to go into a different configuration; the generator would be locked in either the all-zeros or the all-ones state. This means that out of the 2^n different **n**-tuple states an odd tap arrangement would permit only $2^n - 2$ **n**-tuples. Since a maximal length sequence must be $2^n - 1$ bits in length, the number of stages employed in the feedback must be even.

The number of maximally long sequences available from an **n**-stage generator has been stated by Birdsall and Ristenbatt [3] as a theorem: "For an **n**-stage register there are exactly $\Phi(2^n - 1)/n$ sequences of maximal length available with proper feedback connections. Here $\Phi(2^n - 1)$ is Euler's phi function and is defined as follows: $\Phi(K)$ is the number of positive integers less than **K** and relatively prime to **K**, including 1; i.e., $\Phi(K)$ is the number of integers less than **K** that have no common factor with **K**."

Consider our three-stage generator in Fig. 1 ($n = 3$). Then $\Phi(2^3 - 1) = \Phi(7)$. The number of positive integers less than 7 and relatively prime to 7 is 6; therefore the number of maximal length sequences is $\Phi(7)/3 = 6/3 = 2$. One connection must always come from the nth stage (3rd stage in this example). We can further express our **n**-stage linear shift register by a polynomial with coefficients that are added and multiplied modulo 2 as shown by Gold [4]. This polynomial can be represented as

$$f(x) = \sum_{k=0}^{n} C_k x^k, \tag{1}$$

where k is the stage number and the coefficient of the x^k term, C_k, is a one or a zero depending on whether or not it is employed in the feedback connections. We can clarify this with a simple example. Figure 1 shows a feedback connection from the mod-2 adder. For this connection we let $k = 0$. We have further connections from stage one and three to the mod-2 adder, for which $k = 1$ and 3, and by Eq. 1 we have

$$f(x) = x^0 + x^1 + x^3 = 1 + x + x^3.$$

There will always be a term for $k = 0$, because it is the output of the feedback adder.

The significance of having a polynomial to represent the shift register is that when one performs the long division of $1/f(x) = h_0 + h_1 x^1 + h_2 x^2 \ldots h_n x^n$, the coefficients $h_0, h_1, \ldots$ are the terms of the binary sequence generated at the output. Also, according to Gold [4]: "A necessary and sufficient condition that an n-stage shift register generate a maximal sequence of period $2^n - 1$ is that the feedback taps can be connected so that the representing polynomial is primitive. A polynomial $f(x)$ of degree n is primitive if it divides $1 + x^{2^n-1}$ but no polynomial of the form $1 + x^p$ for $p < 2^n - 1$." This theorem is in keeping with our previous condition that one connection must come from the nth stage, for otherwise we would not have a polynomial of degree n and hence could not generate a maximum sequence.

In Fig. 1 our polynomial is $f(x) = 1 + x + x^3$. This divides $1 + x^7$ and therefore will generate a maximum length sequence. We can show this by loading our generator with any configuration except all zeros. If we assume that we load our generator in Fig. 1 with 001; then the successive states along with the initial load become: 001, 100, 110, 111, 011, 101, 010 and starts over again at 001. The output sequence as seen from stage 3 is 1001110, and it is $2^3 - 1$ bits long. We notice that we have $2^3 - 1$, 3-tuple binary numbers that represent all possible states except the all-zero state. Furthermore, all of the 3-tuple binary states can be found in the sequence string 1001110.

An additional property of importance in maximal length sequences is the *shift and add* property. This property means that if a sequence is added modulo-2 to a nontrivial cyclic shift of itself, the resulting sequence is a shifted version of the original. If we express our sequence string as $x(t)$, then the *shift and add* property can be stated as*

$$x(t) \oplus x(t + \tau_1) = x(t + \tau_2). \tag{2}$$

* The symbol $\oplus$ means modulo-2 addition.

We can check our three postulates A, B, and C to see if our generated sequence has these properties. Checking postulate A (balance), our sequence 1001110 contains four ones and three zeros, and their difference is exactly one. To satisfy postulate B (runs) there are four runs, half of length one, one-fourth of length two. Smaller fractions are meaningless in this short sequence. Postulate C (correlation) is closely related to Eq. 3, which is just another way to state postulate C.

We have thus far defined what maximal sequences are, established their general properties, and shown how many maximal length sequences can be obtained from a given n-degree shift register, how to select the taps for maximal length sequences, and how to express our sequence in the form of a polynomial.

Shift Register Length (n)	Taps Used in Mod-2 Feedback		Pseudo-Random Sequence Length ($2^n - 1$)
9	4	9	511
10	3	10	1,023
11	2	11	2,047
12	1 4 6	12	4,095
13	1 3 4	13	8,191
14	1 3 5	14	16,383
15	1	15	32,767
16	2 3 5	16	65,535
17	3	17	131,071
18	7	18	262,143
19	1 2 5	19	524,287
20	3	20	1,048,275

Fig. 3 – Table of taps for various shift register lengths to generate corresponding maximal length sequences.

The guidelines we have established on maximal length sequences will enable us to set up a basic generator of any length and reduce considerably the difficulties normally encountered in picking the proper connections. We will look at some additional properties of PN sequences and subsequently perform some experiments on a few selected sequences. A more detailed analysis on the properties of maximal and nonmaximal length sequences can be found in Refs. 2, 3, and 4.

Our ensuing experiments with PN sequences will come from a PN generator with a shift register capable of being varied from a length of nine bits to a length of 20 bits. There will be only one maximum length sequence considered for each length of the register used. The table for the taps used in this analysis, along with the length of sequence

generated, is given in Fig. 3. The tap numbers correspond to the particular stages of the shift register employed in the modulo-2 feedback. Notice that some sequence lengths required four taps. In these cases a maximum length sequence could not be obtained from two taps.

CORRELATION

The autocorrelation function is one of the most important properties associated with maximum length sequences. The autocorrelation function is approximately zero outside its narrow peak at zero tau, and this holds for all maximum length PN sequences. The sequences are periodic every $2^n - 1$ bits, making the autocorrelation function periodic every $2^n - 1$ bits.

We have tacitly assumed up to this point what correlation means; we will clarify this. Correlation is a measurement of the relationships between two functions and provides another method of statistical measurement. Autocorrelation is a measurement of similarity between delayed replicas of identical functions and crosscorrelation is a measurement of similarity between two nonidentical functions. Correlation can be applied to periodic, aperiodic, or random functions.

The time autocorrelation function for a real function $\mathbf{x(t)}$ is defined as

$$\mathbf{R_{xx}}(\tau) = \lim_{T \to \infty} \frac{1}{T} \int_{-T/2}^{T/2} \mathbf{x(t)\, x(t + \tau)\, dt}. \tag{3}$$

When $\mathbf{x(t)}$ is periodic, as in the case of the maximum length sequences, no limiting process is necessary, and the autocorrelation becomes

$$\mathbf{R_{xx}}(\tau) = \frac{1}{T} \int_{-T/2}^{T/2} \mathbf{x(t)\, x(t + \tau)\, dt}. \tag{4}$$

Two basic properties of the autocorrelation function follows from Eq. 4. First, $\mathbf{R_{xx}}(\tau)$ is an even function. This can be shown by a change of variable in Eq. 4. Let $\mathbf{t' = t + \tau}$; then,

$$\mathbf{R_{xx}}(\tau) = \frac{1}{T} \int_{-T/2}^{T/2} \mathbf{x(t' - \tau)\, x(t')}\, dt' = \mathbf{R_{xx}}(-\tau). \tag{5}$$

The second property is that the autocorrelation function evaluated at $\tau = 0$ is the mean square value of the function $\mathbf{x(t)}$, namely,

$$\mathbf{R_{xx}}(0) = \frac{1}{T} \int_{-T/2}^{T/2} x^2(t)\, dt, \tag{6}$$

and is not exceeded by the absolute value at any $\tau \neq 0$, namely,

$$\mathbf{R_{xx}}(0) \geq |\mathbf{R_{xx}}(\tau)|.$$

We have made no mention up to this point about what the shift rate would be for our sequence generator. We will designate the shift rate as $\mathbf{f_s}$ in bits per second, and the bit interval will be Δt seconds in duration. With the application of isomorphic groups the autocorrelation function for maximum length sequences is shown in Appendix A to be

$$\mathbf{R_{xx}}(\tau) = \begin{cases} 1 - |\tau| \dfrac{2^n}{2^n - 1}, & \text{for } |\tau| \leq 1 \text{ bit} \\ -\dfrac{1}{2^n - 1}, & \text{for } |\tau| \geq 1 \text{ bit} \end{cases} . \tag{7}$$

This will generate a normalized autocorrelation function as shown in Fig. 4. Notice also that we have a peak at integral multiples of the sequence period $2^n - 1$ (clock periods), and beyond one clock (bit) period the correlation is essentially zero for large values of n.

Another way to express the correlation for maximum length sequences is by the correlation coefficient (normalized). The expression for the autocorrelation coefficient is given by

$$\rho_{xx} = \frac{\text{number of agreements} - \text{number of disagreements}}{\text{number of agreements} + \text{number of disagreements}}, \tag{8}$$

where $|\rho_{xx}| \leq 1$.

We have defined the autocorrelation as a measurement of similarity between delayed replicas of identical functions and also stated that crosscorrelation is a measurement of similarity between two nonidentical functions. We can express the crosscorrelation of two real periodic time functions $x(t)$ and $y(t)$ as

$$\mathbf{R_{xy}}(\tau) = \frac{1}{T} \int_{-T/2}^{T/2} x(t)\, y(t + \tau)\, dt. \tag{9}$$

Unlike the autocorrelation function the crosscorrelation function is not an even function. Furthermore, the crosscorrelation function is not necessarily a maximum at tau

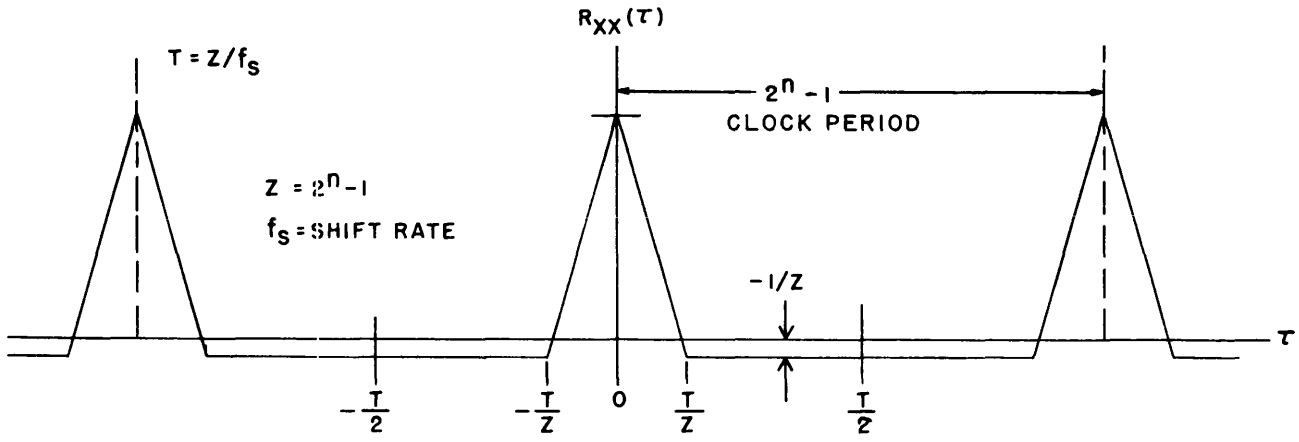

Fig. 4 – Autocorrelation function of a maximal length sequence

zero. As with autocorrelation, crosscorrelation tends to zero as the displacement tends to infinity in either direction; that is

$$R_{xy}(\pm\infty) = 0.$$

POWER SPECTRUM

The experiments to be performed on our PN signals will be analyzed to find out what effects they will have on the power spectrum of the signal. It has been suggested by Blackman and Tukey [1] that the power spectrum of a signal will yield meaningful information where other analysis may fail to give anything significant. By application of the Wiener-Khintchine theorem, it is possible to obtain the power spectrum of PN signals by Fourier transform of the autocorrelation function. The power spectrum as derived in Appendix B (Eq. B24) is

$$W_x(f) = \frac{1}{Z^2}\,\delta(f) + \sum_{\substack{n=-\infty \\ n\neq 0}}^{\infty} \frac{Z+1}{Z^2}\left(\frac{\sin n\pi/Z}{n\pi/Z}\right)^2 \delta\left(f - \frac{nf_s}{Z}\right), \tag{10}$$

where $Z = 2^n - 1$ is the number of bits in the sequence and f_s is the shift frequency in bits per second.

The Dirac delta function $\delta(f)$ as explained in Appendix B can be thought of as a *sifting* function, such that it has unit area and is zero for all nonzero values of its argument.

The expression for the power spectrum has some interesting aspects to it that deserves further comment. The first term in the equation pertains to the energy associated in the neighborhood of the zero frequency component and is essentially zero for any sequence that is long. Since $1/Z^2$ becomes insignificant when $n \geq 10$, the minimum value of n dealt with in this thesis will be 10.

The second term, containing $[(\sin n\pi/Z)/(n\pi/Z)]^2$ will create an envelope around the discrete line frequencies and will always be positive and real. The Dirac delta function multiplying the sine-squared term will generate the discrete line spectrum with frequency components every f_s/Z Hz and would have a constant height of $(Z + 1)/Z^2$ were it not for the modulating sine term. Another interesting effect that takes place is the occurrence of nulls at integral multiples of the shift frequency f_s. These nulls are created because $\sin n\pi/Z$ is zero for every value of n that is a multiple of Z and since in the argument of the delta function this ratio of n/Z multiples f_s, our nulls appear at integral multiples of the shift frequency. The bandwidth of the spectrum is also dependent on f_s and its width

out to the half-power points gives a bandwidth of $W_x(f) \approx 0.32\ f_s$, where the constant term 0.32 is the approximate multiplication factor for the -3 db-down point.

One further noteworthy point about PN sequences is the time period associated with the sequence. We have spoken of the bit length and shift rate without combining these two effects to establish the PN time period. The inversion of the term f_s/Z in the equation of the power spectrum is the time period of the PN sequence and will be designated as $P = Z/f_s$, the period in seconds of a given PN sequence.

Measurement of Power Spectrum

The first phase of our experiment will be a laboratory measurement of the power spectrum to see how close we are in agreement with the mathematical model of the power spectrum.

When building a PN generator one would like to know how fast it should be shifted or whether there is an optimal shift rate for a given sequence length that should be considered. Since there does not seem to be any mathematical basis for checking the output power level as a function of shift rate and sequence length, this test becomes a logical starting point in the experiment.

The PN generator employed in this and all subsequent tests is a variable length generator with a shift register that can be varied from a length of nine bits to a maximum of 20 bits and will generate the sequence lengths tabulated in Fig. 3. The logic for the generator was made up of Navigation Computer Corporation 300-kHz modules and driven by a Hewlett-Packard 5100A frequency synthesizer. The frequency synthesizer is driven by a 5100A synthesizer driver and will provide any output frequency from 0.01 Hz to 50 MHz, selectable in steps as small as 0.01 Hz. The high stability of the 1-MHz basic crystal (3 parts in 10^9 for 24 hours) makes an excellent standard for laboratory experiments.

A check of the output power in decibels versus shift rate on a maximal length sequence revealed that the output was essentially constant for all maximal sequence lengths that could be generated by our generator and was invariant to the shift rate. These preliminary results are in keeping with our assertion that the sequence has uniform power throughout its bandwidth. It will be subsequently shown that the bandwidth is independent of the sequence length and is determined solely by the shift rate, i.e., how often the waveform switches.

Output Power Versus Frequency

When selecting PN sequences as a signal source, the question of what shift rate should be employed will be of some concern. The shift rate will determine the bandwidth of the signal and can be roughly estimated, but the behavior of the power spectrum of PN sequences may not be readily understood, and the effects of using various shift rates may not be apparent. In some applications of PN signals it must be bandlimited (such as sonar signals) and as a result it would be instructive to get a plot of the power spectrum of the wideband signal before applying any filters.

The test procedure for obtaining the frequency response output of the PN signal was as follows. A Hewlett-Packard frequency synthesizer was used to drive the PN generator, and the output of the generator was fed to a Muirhead-Pametrada Type D-489-E wave analyzer. The Muirhead analyzer is of the degenerative feedback type employing two selective amplifiers in cascade. The output at the tune frequency is fed through a further amplifier to the meter. Tuning is by resistance-capacitance networks, and the tuning of the two amplifiers can be staggered to give a bandpass effect. The analyzer was operated in the *IN Tune High* position, so that both selective amplifiers are in the circuit and tuned to the same frequency, giving a **Q**-factor of 80 and an octave discrimination of better than 70 dB.

Tabulating the decibel output versus frequency for various fixed shift rates and all maximal length sequences obtainable from our PN generator, a composite graph was plotted for output versus frequency and is shown in Fig. 5. Values less than 150 Hz could not be obtained due to a coupling capacitor in the PN generator that blocked these lower frequencies. Figure 5 shows that there is a frequency null at integer multiples of the shift rate frequency $\mathbf{f_s}$ and that the spectrum was the same for all maximal length sequences that could be obtained from our generator. Although the nulls were not zero, they were 15 to 25 dB below the average value and each corresponding peak. The graph is in excellent agreement with that of Allen and Westerfield [5] except where the spectrum starts to roll off. This difference in roll-off, may be attributed to shape of the square waves generated at the output of our respective units; i.e., the squareness of the output pulses will have some effect on the spectrum.

The interesting thing about the graph is that it depicts pictorially what is inherent in Eq. 10. The graph is drawn smooth rather than as discrete line frequencies because it is a composite of virtually any shift rate and any sequence (maximal) length. The spectrum plot enables one to select a particular bandpass filter where the power is essentially constant and to avoid the areas where the nulls occur.

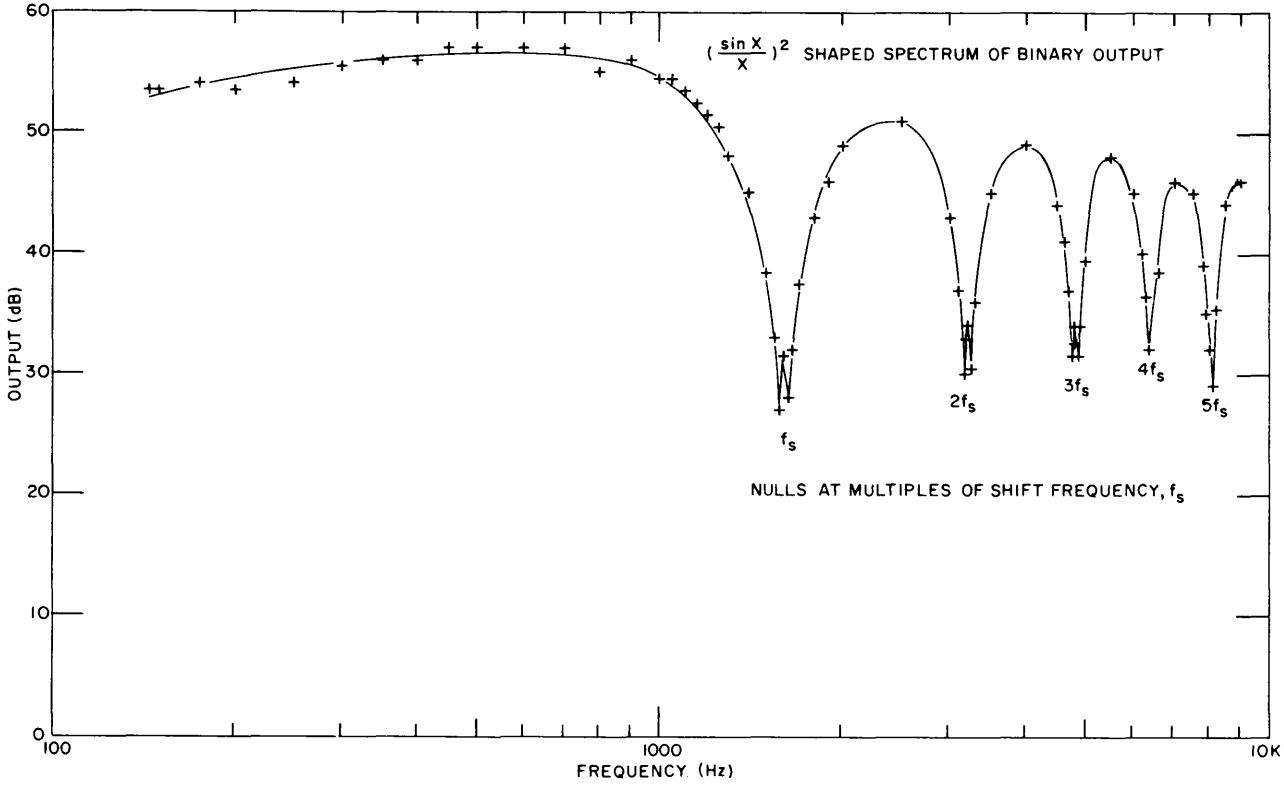

Fig. 5 – Power spectrum of wideband pseudo-random noise

BANDWIDTHS

A function cannot be limited in both the time and frequency domains. There is a duality in nature between time, whose dimension is **t**, and frequency **f**, whose dimension is 1/t. A precise determination of frequency requires a long time base, and conversely a precise determination of time requires a broad frequency band.

The dual assumption that the sample record **f(t)** can exist for a finite time interval from 0 to **T** seconds, and its Fourier transform $\mathbf{F}(\omega)$ exists only in a frequency interval from $-\mathbf{W}$ to $+\mathbf{W}$ Hz is not theoretically possible because of an *uncertainty principle* [6]. Assuming **f(t)** and $\mathbf{F}(\omega)$ are so restricted as to their time and frequency properties, it will be shown in the section on sampling analysis how many distinct samples of **f(t)** or $\mathbf{F}(\omega)$ are required to describe **f(t)** completely for all **t**.

In actual practice, we can closely approximate this dualty with finite time intervals and bandpass filters. For a bandlimited signal the Fourier transform $\mathbf{F}(\omega)$ corresponding to **f(t)** vanishes identically for all real ω outside some specified band. In the case of a *low-pass* signal where $\mathbf{W}$ is the highest frequency (Hz) appearing in the signal we can specify our band for all real ω as being $-2\pi\mathbf{W} \leq \omega \leq 2\pi\mathbf{W}$ for $\mathbf{W} > 0$, and this would imply that

$$|\mathbf{F}(\omega)| = 0 \qquad \text{for } |\omega| > 2\pi\mathbf{W}. \tag{11}$$

The total bandwidth would be equal to $4\pi\mathbf{W}$ Hz centered about the zero frequency component. A *bandpass* signal is defined in the same way as the low-pass signal, except the boundaries of ω are different. If ω_0 is the center frequency of our band, then the range of the *bandpass* signal can be given by

$$\omega_0 - \frac{\Omega}{2} \leq \omega \leq \omega_0 + \frac{\Omega}{2} \tag{12}$$

and

$$-\omega_0 - \frac{\Omega}{2} \leq \omega \leq -\omega_0 + \frac{\Omega}{2}.$$

This means that $|\mathbf{F}(\omega)| = 0$ for $|\omega| \geq \omega_0 + \Omega/2$.

The important concept about bandlimited functions is that they are zero outside the band. It is not possible in a practical case to get a time function whose Fourier transform vanishes identically outside some specified band. Generally, we assume that the Fourier transform is very small outside some finite interval.

Bendat and Piersol [6, Ch. 6] describe three types of bandwidths that are of interest to the power spectral density measurement problem. These three bandwidths are the

half-power-point bandwidth $\mathbf{B_r}$, the *noise* bandwidth $\mathbf{B_n}$, and the equivalent statistical bandwidth $\mathbf{B_s}$.

The half-power-point bandwidth $\mathbf{B_r}$ is the frequency interval between the upper and lower frequencies where the filter attenuates the applied signal by 3 dB below that of maximum transmissability. The half-power bandwidth is convenient due to its ease of measurement and is represented by

$$\mathbf{B_r} = \mathbf{f}_2 - \mathbf{f}_1, \tag{13a}$$

where

$$|\mathbf{H}(\mathbf{f}_1)|^2 = |\mathbf{H}(\mathbf{f}_2)|^2 = \frac{1}{2}|\mathbf{H_m}|^2. \tag{13b}$$

$\mathbf{H}(\mathbf{f})$ is the frequency response function of a linear filter. $|\mathbf{H}(\mathbf{f})|$ is the magnitude of the frequency response function (gain factor) at any frequency $\mathbf{f}$ and $|\mathbf{H_m}|$ is the maximum value of the gain factor.

The noise bandwidth $\mathbf{B_n}$ is the bandwidth of a hypothetical rectangular filter which would pass a signal with the same mean square value as the actual filter when the input is white noise (random signal with uniform energy distributed over all frequencies). Noise bandwidth $\mathbf{B_n}$ can be defined as

$$\mathbf{B_n} = \int_0^\infty \frac{|\mathbf{H}(\mathbf{f})|^2\, \mathbf{df}}{|\mathbf{H_m}|^2}. \tag{14}$$

The equivalent statistical bandwidth $\mathbf{B_s}$ is the bandwidth of a hypothetical rectangular filter which would pass a signal with the same mean-square-value statistical error as the actual filter when the input is white noise and is defined as

$$\mathbf{B_s} = \frac{\left[\int_0^\infty |\mathbf{H}(\mathbf{f})|^2\, \mathbf{df}\right]^2}{\int_0^\infty |\mathbf{H}(\mathbf{f})|^4\, \mathbf{df}}. \tag{15}$$

In actual practice there is very little difference between these three types of filters, provided one is using a highly selective bandpass filter that closely approximates the ideal rectangular form. We can only assume that ideal filters will give us exact bandwidths. The consideration of theoretical rectangular filters (unity gain within the passband) is a mathematical artifice that enables us to use the sampling theorem.

SAMPLING ANALYSIS

The concept of bandwidths is useful in a mathematical treatment of sampled signals, and in a practical sense transmission of information is more economical when bandwidth is conservative.

The Shannon *Sampling Theorem* states [7]: "If a function $f(t)$ contains no frequencies higher than W Hz, it is completely determined by giving its ordinates at a series of points spaced $1/2W$ seconds apart." Stated mathematically the theorem becomes

$$f(t) = \sum_{-\infty}^{\infty} f\left(\frac{n}{2W}\right) \frac{\sin 2\pi W\left(t - \frac{n}{2W}\right)}{2\pi W\left(t - \frac{n}{2W}\right)}. \tag{16}$$

Equation 16 shows that a time function $f(t)$ can be completely determined by its sample points $(n/2W)$. Since $f(t)$ contains no frequencies higher than W Hz, it cannot change to a substantially new value in a time less than one-half cycle of the highest frequency, i.e., $1/2W$. Shannon's proof of this sampling theorem is given in Ref. 7 and repeated here due to its simplicity.

"Let $F(\omega)$ be the spectrum of $f(t)$. Then

$$f(t) = \frac{1}{2\pi} \int_{-\infty}^{\infty} F(\omega)\, e^{j\omega t}\, d\omega = \frac{1}{2\pi} \int_{-2\pi W}^{2\pi W} F(\omega)\, e^{j\omega t}\, d\omega, \tag{17}$$

since $F(\omega)$ is assumed zero outside the band W. If we let

$$t = \frac{n}{2W}, \tag{18}$$

where n is any positive or negative integer, we obtain

$$f\left(\frac{n}{2W}\right) = \frac{1}{2\pi} \int_{-2\pi W}^{2\pi W} F(\omega)\, e^{j\omega \frac{n}{2W}}\, d\omega. \tag{19}$$

On the left are the values of $f(t)$ at the sampling points."

The validity of this proof lies in the fact that the integral on the right is the nth coefficient in a Fourier-series expansion of the function $F(\omega)$, taken on the interval $-W$ to $+W$. The values of the samples $f(n/2W)$ determine the Fourier coefficients in the series expansion of $F(\omega)$; thus they determine $F(\omega)$. Since $|F(\omega)| = 0$ for $|\omega| > W$, $F(\omega)$ is determined if its Fourier coefficients are determined. By the *uniqueness* of Fourier transforms (see Eqs. B4 and B7) only one function can have a particular transform $F(\omega)$; hence $f(t)$ is completely determined by its samples taken every $1/2W$ seconds apart.

More elaborate proofs on the *Sampling Theorem* can be found in the literature dealing with sampled data. It shall suffice at this point to say that the techniques of sampling data has extensive application in communication systems and areas where digital computers are employed. The use of digital computers will require that time functions be represented by sampled data points.

The analysis in this thesis has been performed with the aid of a digital computer on sampled data points taken from a PN generator. By thinking of the PN signal as being bandlimited to a bandwidth **W** and some time interval **T**, we can completely specify our time function **f**(t) by 2**TW** numbers.

These 2**TW** numbers are the degrees of freedom that represent the original time function. Our 2**TW** samples are obtained by equally spaced sampling. According to Shannon these samples may be unevenly spaced, but the reconstruction process is more involved with unequal spacing. The value of the function can be also determined by sampling at half the prescribed sampling rate and taking the derivative, or by sampling at a third of the rate and taking both first and second derivatives at these sampled points. In short, any set of 2**TW** independent numbers associated with the function can be used to describe it.

FILTERING

Our previous discussions about bandwidths, and sampling of bandlimited functions, dealt with theoretical bandwidths with very sharp cutoffs. In actual practice there is some departure from the ideal bandwidth where the frequency spectrum is identically zero outside the band as described by Eqs. 11 and 12.

The usual method employed in obtaining bandlimited functions is with some appropriate type of filtering. Winder and Loda [8] discuss various types of filtering and some methods used in obtaining the filtering. The more rigorous details of filtering and their effects will not be undertaken in this report, since filtering comprises a complex area of study on its own.

This study of PN signals will deal almost exclusively with low-frequency (less than 1 kHz), bandlimited signals that have undergone some type of corruption. We have restricted our signals to the lower frequencies because this is the range generally used for long-range underwater acoustic transmission. These low-frequency signals are bandlimited both to match the frequency response of the transducer and to minimize dispersion (velocity spread of the different frequencies).

The filters used in this study are of the commercial variety and do not possess the characteristics of an ideal rectangular-bandpass filter, nor do they lend themselves to any known mathematical models of bandpass filters.

One filter that has been used in this study is a Krohn-Hite Model 330-A *Ultra-Low-Frequency* bandpass filter. It is an adjustable filter whose gain is unity in the passband and drops off at a rate of 24 dB/octave outside the passband. Both the high and low cut-off frequencies are independently adjustable from 0.02 to 2000 Hz. This filter is superior to a 24-dB filter with unity peaking, because with the same attenuation outside the passband, the gain near the corner frequencies is greater due to employment of corner peaking.

The second type of filter employed in this study is a Burnell filter that is not adjustable but comes in various bandwidths for a given center frequency. The filter bandwidths are expressed as a percent of the center frequency such that a 400-Hz 30-percent filter is centered at 400 Hz with a bandwidth of 120 Hz. The Burnell filters drop off at a rate of 55 to 65 dB/octave outside the passband and are not maximally flat within the passband but display an equi-ripple passband characteristic. Although the Burnell filters do not have unity gain within the passband, they exhibit more than twice the attenuation rate per octave than the Krohn-Hite filters. The sole purpose of using filters as far as this study is concerned is to limit the signal to a frequency band that fits a particular system. The filters will not perform any preprocessing of the signals such as predicting, smoothing, and correlating; all processing will be handled by the computer.

PN SIGNATURE

The logical starting point on the investigation of power spectral estimates of sampled data is to find what type of *signature* the PN possess under normal conditions. A PN model suitable for our studies will be undertaken first, and consideration will be given to the following parameters: PN period (seconds), bandwidth (Hz), sampling rate (bits per second), computer program resolution for power density (Hz), harmonic separation of PN (Hz), and the number of sample points per PN period.

We shall discuss the meaning of the terms used above as they apply to this investigation. The PN period in seconds is a function of the sequence length and shift rate such that the period $p = Z/f_s$, where $Z = 2^n - 1$ bits and f_s is the shift rate in bits per second. The period of the PN must be restricted so that a full sequence length of the sampled signal can be accommodated in the computer memory. The significance of this consideration about the PN sequence length will be borne out in later developments.

Long PN sequences when filtered have distributions that are almost Gaussian and therefore more desirable for some applications.

A compromise on the PN sequence length must be made or it will require a high shift rate to hold the PN period to a few seconds. If a PN of 2 seconds were considered and a sampling rate of 2000 Hz were used, this would give 4000 data points to cover one period of the PN, which would be too much data for the computer used in this analysis. Although the upper frequency of the bandwidth is about 450 Hz, the sampling rate is higher than that required by the sampling theorem, but this higher rate gives better coverage of the signal and minimizes the need for interpolation between data points.

The bandwidths used on the PN in this study will generally be 100 Hz wide centered at either 200 Hz or 400 Hz. The filtered PN is sampled and encoded using the NRL [9] magnetic digital recording system. The system is capable of eight-channel multiplexing but is used in a single-channel mode in this report. Essentially the recording system will sample the analog signal at some designated rate and encode the instantaneous value of voltage into binary digits consisting of ten bits and sign. The 11-bit data word is recorded on tape along with a parity bit and clock bit, this process being repeated for each sample point. This recording system has a maximum sampling rate of 8 KHz and also incorporates a visual monitor (Fig. 6). The visual monitor serves as a very useful device for inspecting the data after it is written on tape.

The computer used in this report is a Computer Control Company DDP-24 high-speed, solid-state, general-purpose digital computer. The computer has a 24-bit word length and uses standard IBM character format for its input-output tape units. The model used in this report has a 4096-word memory expandable to 32,768 words. The total memory capacity at present of 4096 words will dictate selection of the length of the PN period. The computer memory will be required to hold the power spectrum program along with appropriate subroutines and enough data to cover a minimum of one full PN period.

COMPUTER PROGRAM

The program for computing the power spectrum is part of the standard library of programs available for IBM compatible computers. We will not attempt to go through the algorithms associated with the computer handling of the power spectrum except to outline briefly the more important aspects of it. Some standard methods for computer computation can be found in Ralston and Wilf [10]. The program handles the calculation of the power spectrum using the following method.

First we consider a time series with zero mean and define an autocovariance function $W(\tau)$ as

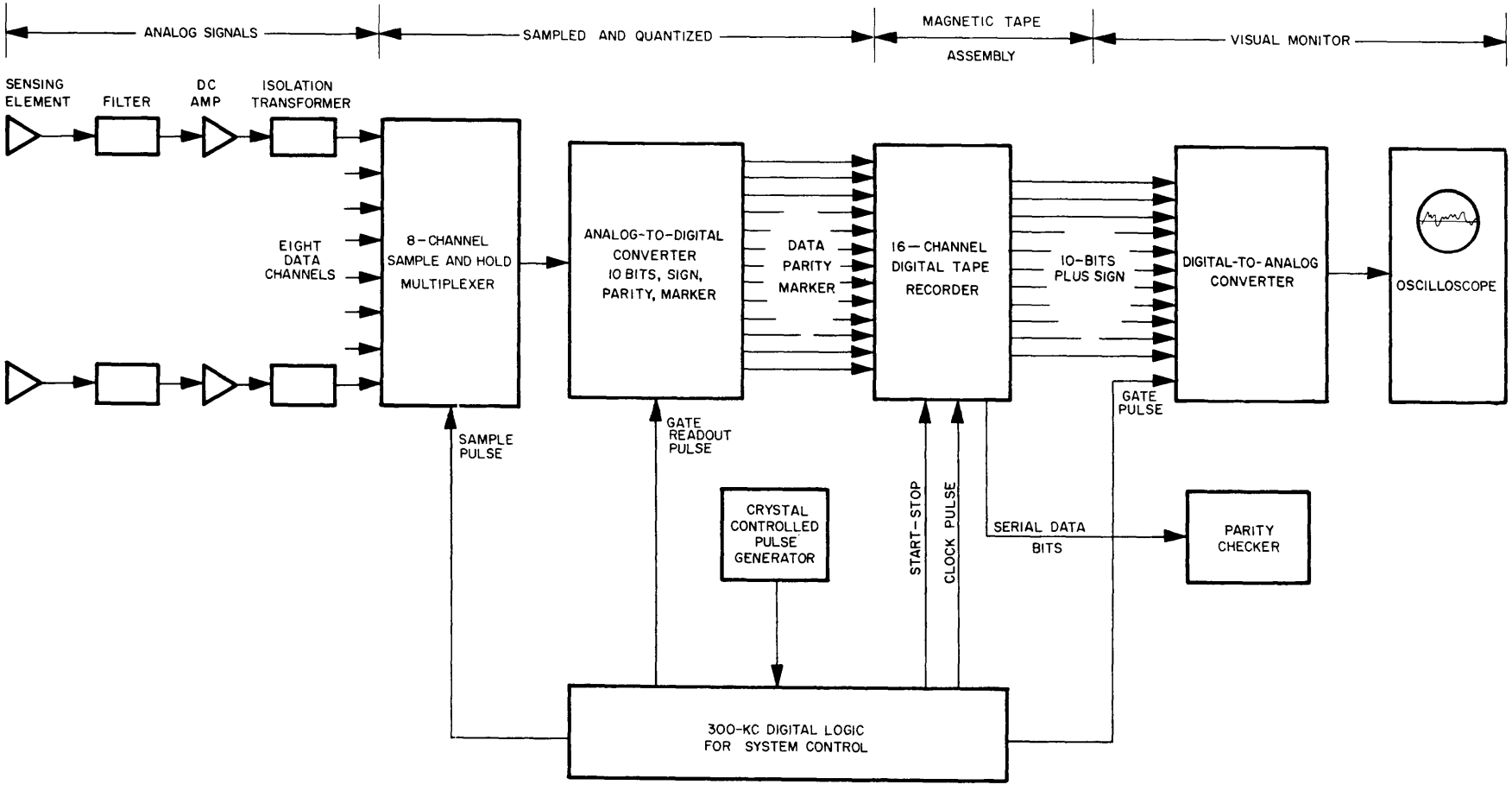

Fig. 6 – Digital recording system with eight channels of multiplexing

$$\mathbf{W}(\tau) = \frac{1}{N - \tau} \int_{i=1}^{N-\tau} x_i \; x_{i+\tau}, \tag{20}$$

where τ is the lag between observations, N is the total number of observations, and x_i is an individual observation. The autocovariance function described by Eq. 20 is for a discrete time function, and since we are assuming a time series with zero mean, the autocorrelation function will be the same as the autocovariance function.

Recalling that the autocorrelation function and power spectrum are Fourier transforms of each other (Appendix B, Eqs. B19), we can express the power spectrum in terms of the autocovariance function. If $\mathbf{x}(t)$ is real, $\mathbf{W}(\tau)$ is real and symmetric around $\tau = 0$. Therefore $\mathbf{W}(\tau)$ and $\mathbf{P}(\mathbf{f})$ may be expressed as two-sided cosine transforms:

$$\mathbf{W}(\tau) = \int_{-\infty}^{\infty} \mathbf{P}(\mathbf{f}) \cos 2\pi \mathbf{f} \tau \; \mathbf{df}, \tag{21a}$$

$$\mathbf{P}(\mathbf{f}) = \int_{-\infty}^{\infty} \mathbf{W}(\tau) \cos 2\pi \mathbf{f} \tau \, \mathbf{d}\tau, \tag{21b}$$

or more simply as

$$\mathbf{W}(\tau) = 2 \int_{0}^{\infty} \mathbf{P}(\mathbf{f}) \cos 2\pi \mathbf{f} \tau \; \mathbf{df}, \tag{22a}$$

$$\mathbf{P}(\mathbf{f}) = 2 \int_{0}^{\infty} \mathbf{W}(\tau) \cos 2\pi \mathbf{f} \tau \; \mathbf{d}\tau. \tag{22b}$$

Equations 21 and 22 are used in place of the usual exponential form for convenience of future developments, and the justification for this cosine transform lies in the fact that the autocorrelation function is an even function and the sine terms are zero. The power spectrum associated with only positive frequencies would be equal to twice the $\mathbf{P}(\mathbf{f})$ given in the above equations.

Since we are dealing with a discrete set $\mathbf{x}_i(t)$, it is necessary to use a finite Fourier series transformation rather than the infinite integral transformation. If the spectrum involves angular frequencies no greater than π, estimates of the spectral density can be given by

$$S_\tau(\mathbf{f}) = \mathbf{W}_0 + 2 \sum_{q=1}^{M-1} \mathbf{W}_q \cos \frac{q\tau\pi}{M} + \mathbf{W}_M \cos \tau\pi, \tag{23}$$

where $W_0, W_1, \ldots, W_M$ are calculated by Eq. 20, **M** is the maximum number of lags, and **q** is a discrete time index.

The raw estimates of spectral power given by eq. 23 are printed out as a function of frequency, $\tau \Delta f$ where τ is incremented by one for each calculation and

$$\Delta f = \frac{f_s}{2M}, \tag{24}$$

in which f_s is the sampling frequency, and **M** is as defined previously. The quantity Δf is essentially the frequency resolution of the program.

The computer program holds 2500 data points, and working with a rule that the tau shifts should not exceed 10 percent of the data points, we get 250 tau shifts for our value of **M**. At $\tau = 0$ (no shift) we get W_0, and the program generates a power component for each tau shift up to a maximum of 250. Our concern with frequency resolution of the computer program is based on a desire to have the computer program resolve frequencies finer than those generated by the PN signal being investigated.

As mentioned earlier four basic parameters to be considered are PN period, bandwidth, sampling rate, and computer program resolution. Our concern with these parameters lies in selecting a PN period with an appropriate bandwidth such that our sampling rate will give at least one full PN period for our 2500 computer data points.

This restriction on the number of data points, dictated by the computer memory size, puts a severe limitation on the period length of the PN. Ideally we would like PN periods of about 1 minute, or more because these would have amplitude distributions more closely approaching Gaussian distributions and would lend themselves to mathematical models already established for the Gaussian case. We are essentially faced with using PN periods that are so short in length that they lose their random characteristics as well as not being Gaussian distributed, and our mathematical models may not fit our actual results.

The compromise between the most desirable signal and limitations imposed on a signal due to the computer hardware represents a rather realistic picture of what one is actually confronted with in a practical situation. This compromise may be summed up as being the difference between what is mathematically elegant and what is physically realizable as far as a given computer is concerned.

EXPERIMENTAL RESULTS

Pseudo-Noise Signature

The first computer experiment in this report involves finding a suitable PN sequence and bandwidth that can serve as a model for the power spectrum estimates. This means

that we will have a PN *signature* of the power spectrum for a given PN sequence and sample size, to be compared to other PN power spectrums after there has been some perturbations of the PN signal.

We start out by selecting three PN sequences generated by shift register lengths of 10, 11, and 12 bits. The sampling rates, shift rates, and bandwidths will be changed until we find a PN sequence with the most desirable looking power spectrum.

Noting from Eq. 24 that the computer program had a frequency resolution given by Δf = sampling rate/2**M**, where **M** = 250 tau shifts, we would like the resolution of the computer to be smaller than the harmonic separation of the PN sequence. The bandwidths were selected for frequency ranges of 150 to 250 Hz and 350 to 450 Hz. These two bandwidths are located before the first null as shown by Fig. 5 and in the region where the power is almost constant over the entire bandwidth of interest.

The block diagram of the recording setup is shown in Fig. 7. A frequency synthesizer (Hewlett-Packard) was used to drive the PN generator at some appropriate shift rate, such that for a given sequence length the harmonic separation is an integral multiple of the computer program resolution. The square waves from the output of the PN generator were fed to a bandpass filter. The filter can be either a 150 to 250 Hz Krohn-Hite bandpass filter or a Burnell 350 to 450 Hz bandpass filter. The output of the filter is taken across a voltage divider before feeding into a wideband dc amplifier. The amplifier serves as an impedance match between the PN generator and the analog-to-digital (A/D) converter and also serves to maintain the voltage level into the converter at full scale. Between the amplifier and the A/D converter is an isolation transformer to block out any dc bias.

The A/D converter is triggered by another frequency synthesizer of the same model used for shifting the PN generator. The trigger pulse into the converter is essentially the sampling rate, and this sampling rate is set to give the computer program a frequency resolution finer than the harmonic separation of the PN generator. The output of the A/D is fed in parallel ten-bits, sign, parity, and clock onto a 16-channel digital magnetic recorder. A total of 18 recordings were made from this arrangement using three different maximal length PN sequences. The values used in this recording are shown in Table 1. The table shows three different sampling rates along with appropriate values of PN shift rates that were used for the 150 to 250 Hz bandwidth and also for the 350 to 450 Hz bandwidth. In all cases the harmonic separation of the PN was at least double the frequency resolution of the program.

The unsmoothed raw estimates of the spectral density were computed using Eq. 23, and the normalized values of the frequency components were plotted. Figure 8a shows the power spectrum of a pseudo-random sequence of length $2^{10}-1$ bits that has been filtered through a bandpass filter of 150 to 250 Hz. Associated with the plot of the

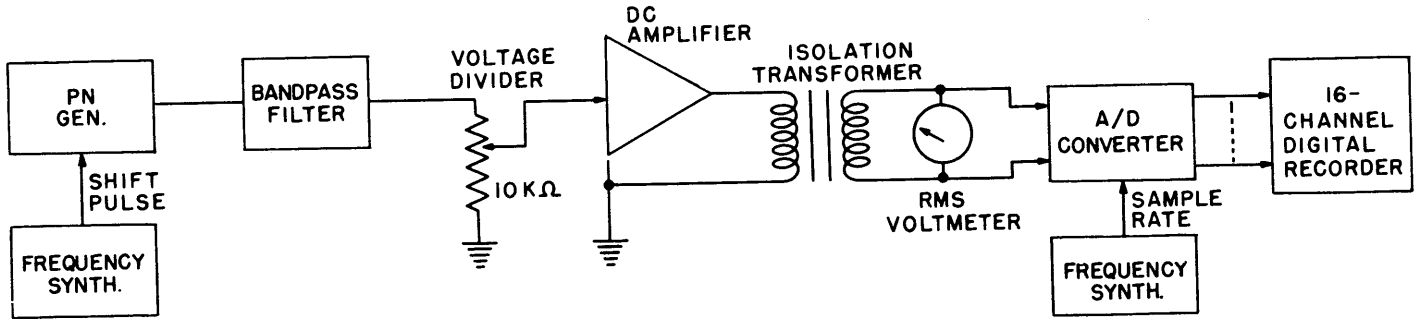

Fig. 7 – Digital recording of PN at various shift rates and sampling rates

spectral density is the corresponding plot of the normalized autocorrelation function, Fig. 8b. Figure 8 represents the data associated with Case 1 of Table 1.

The autocorrelation plot of Fig. 8b shows the very sharp spike at $\tau = 0$ and all multiples of the PN period. These sharp spikes with almost zero side noise between peaks are also in excellent agreement with the literature on maximal length sequences. The small gap between every other maximum value of the correlation was due to the computer bringing in a new block of data while the chart paper was still in motion. The plots of the autocorrelations were made by a Brush two-channel strip recorder (Mark 280) and will be used for comparison with the spectral analysis.

Figures 9a and 9b are the plots of power spectrum and autocorrelation for Case 16 associated with Table 1. The bandwidth in this case was 100 Hz centered at 400 Hz, and a different type bandpass filter was used than that of Fig. 8. The power spectrum is as it should be for filtered PN sequences and all the associated data for it are in Table 1. This filter displayed an equi-ripple characteristic in the bandpass region and had a considerably sharper cutoff outside the passband than that used in the lower frequency case.

The autocorrelation of Fig. 9b is still well defined at $\tau = 0$ and all multiples of the PN period. The development of a $(\sin x)/x$ envelope is better defined in this higher frequency case. This envelope is better developed at this frequency due to the ability of the filter to pass higher frequency excursions and the fact that the bandwidth approaches that of a square wave. The excursions within the $(\sin x)/x$ envelope are essentially at the center frequency of the filter.

Figures 10a and 10b are for PN sequences of $2^{11} - 1$ bits and represent Case 2 from Table 1. It can be noted how the envelope of the power spectrum is not as smooth for the low-frequency bandwidth using this longer PN sequence length as it was for the previous case. This PN sequence exhibits a high ripple component in both frequency bands.

Figures 11a and 11b are for PN of sequence length $2^{12} - 1$ bits. The plots are for Case 3 of Table 1. The most noticeable item of this power spectrum is the considerable power in frequency bands between the harmonic separation of the PN. In other words for the sequence and shift rate used the frequency separation should have been every 8 Hz but instead was every 4 Hz. Since the program had a resolution of only 4 Hz, it is not possible to see how intense this crosstalk really was. The autocorrelation of Fig. 11b remains well defined for all of the in phase values, similar to the previous two cases.

Table 1

Cases Recorded for PN Sequences of Shift Register Lengths 10, 11, and 12

Case	n Shift Register Length	X Sample Rate (Hz)	Δf Computer Program Resolution (Hz)	f PN Harmonic Separation	f_s Shift Rate (Hz)	Sample Points per PN Period	Bandwidth (Hz)
1	10	2000	4	8	8184	250	150-250
2	11	"	"	"	16,376	"	"
3	12	"	"	"	32,760	"	"
4	10	1500	3	6	6138	333.3	"
5	11	"	"	"	12,282	"	"
6	12	"	"	"	24,570	"	"
7	10	1000	2	4	4092	500	"
8	11	"	"	"	8188	"	"
9	12	"	"	"	16,380	"	"
10	10	"	"	"	4092	"	350-450
11	11	"	"	"	8188	"	"
12	12	"	"	"	16,380	"	"
13	10	1500	3	6	6138	333.3	"
14	11	"	"	"	12,282	"	"
15	12	"	"	"	24,570	"	"
16	10	2000	4	8	8184	250	"
17	11	"	"	"	16,376	"	"
18	12	"	"	"	32,760	"	"

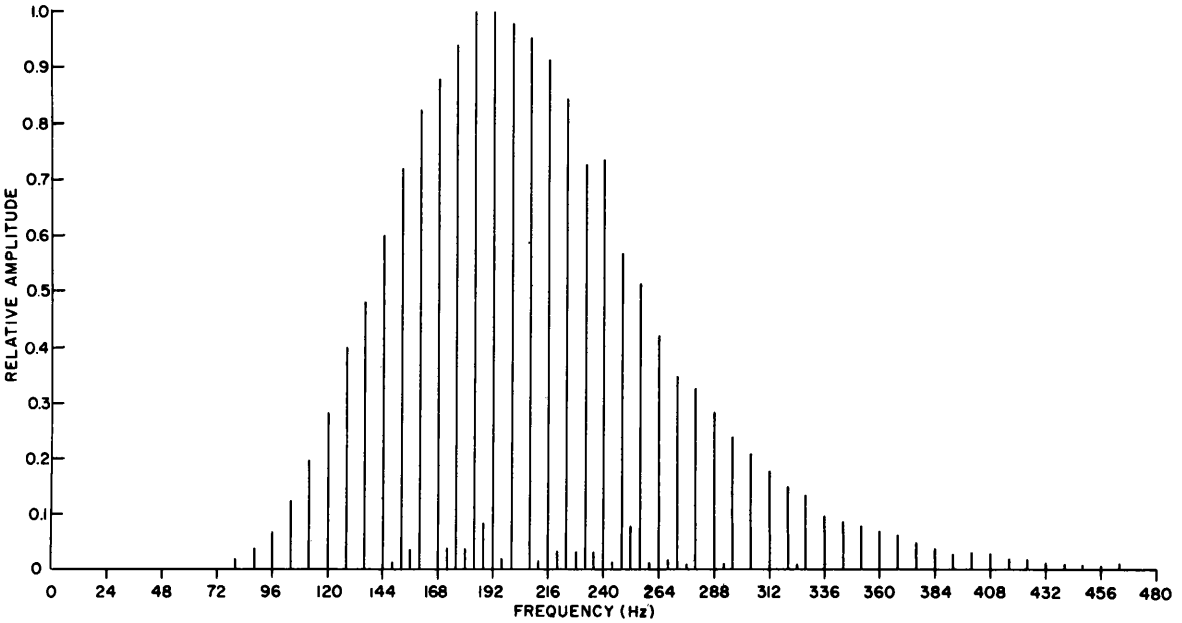

(a) Power spectrum estimates

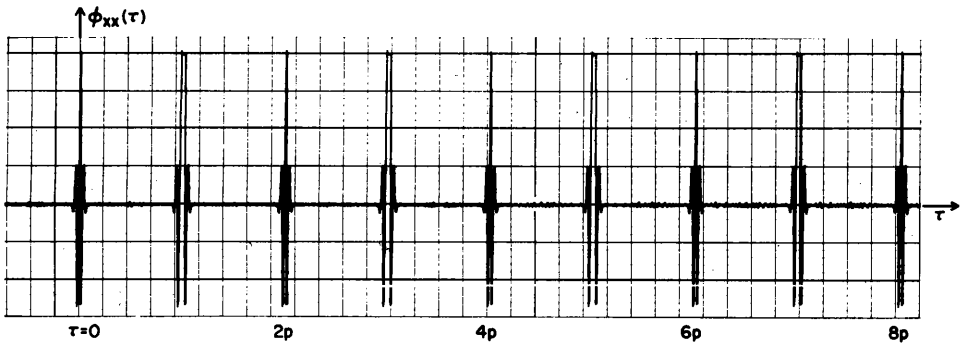

(b) Autocorrelation

Fig. 8 – Power spectrum estimates and autocorrelation of bandlimited PN (Case 1 of Table 1: BW = 150-250 Hz; Z = 1023 bits)

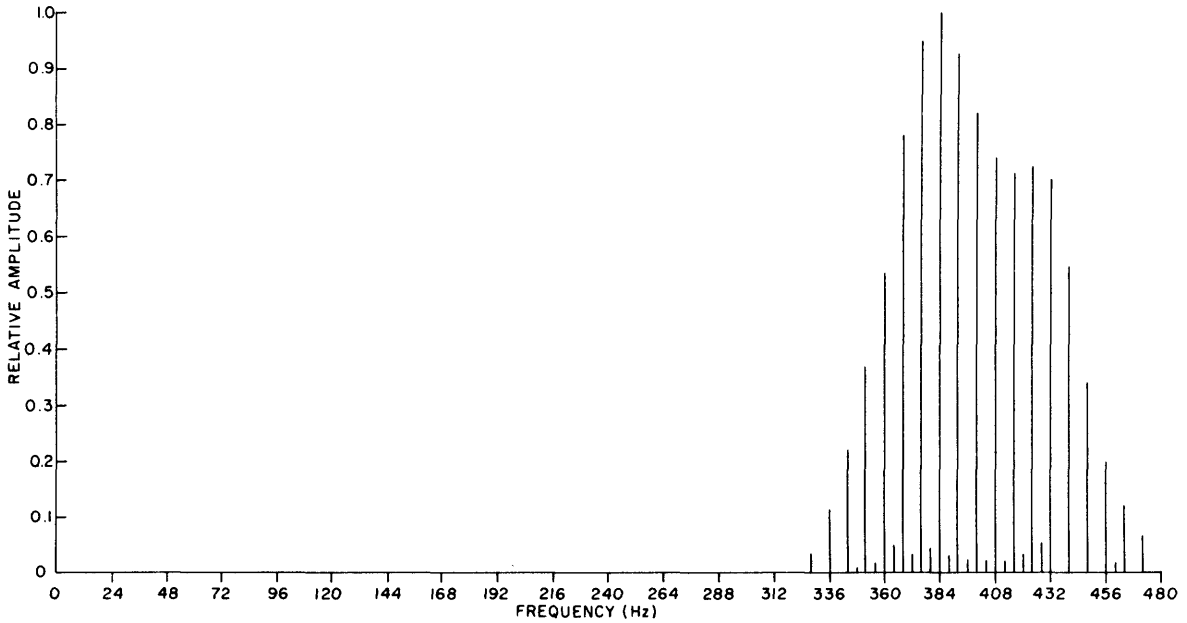

(a) Power spectrum estimates

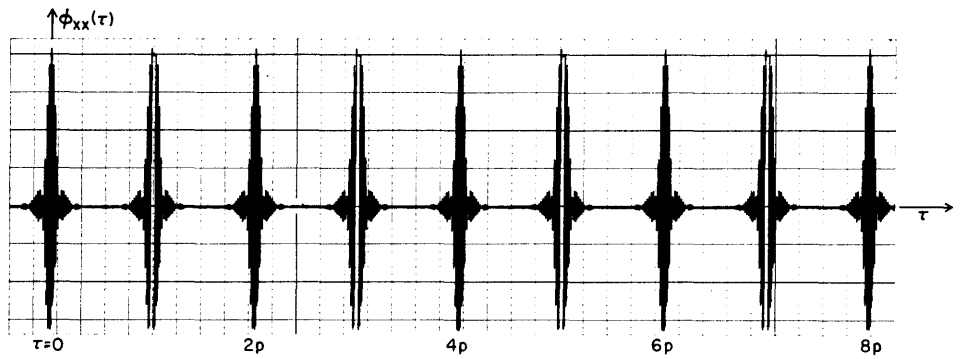

(b) Autocorrelation

Fig. 9 – Power spectrum estimates and autocorrelation of bandlimited PN (Case 16 of Table 1: BW = 350-450 Hz; Z = 1023 bits)

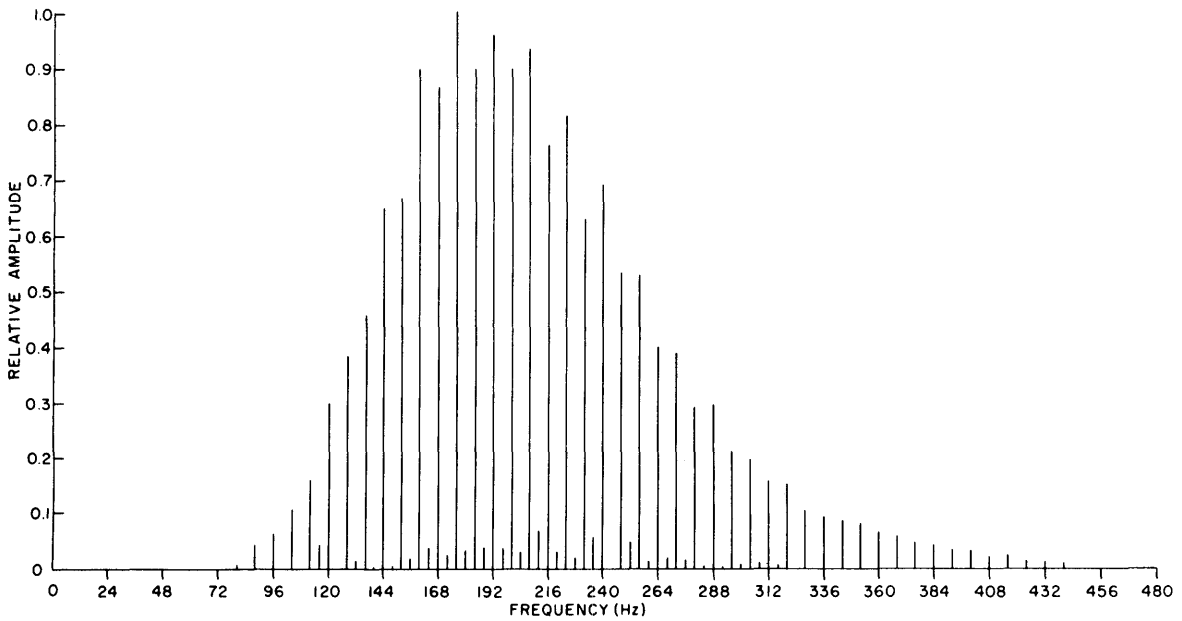

(a) Power spectrum

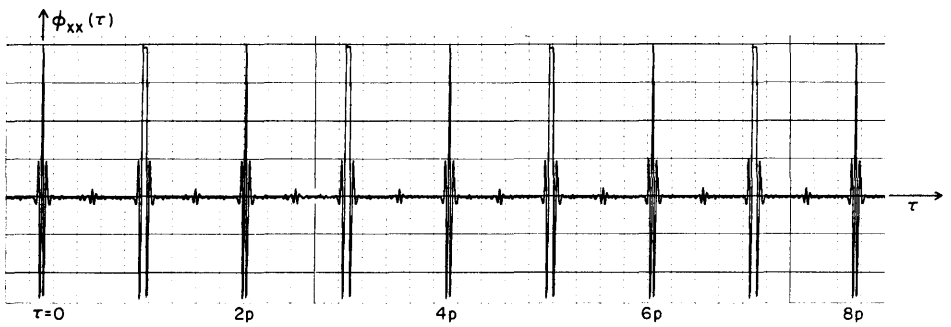

(b) Autocorrelation

Fig. 10 – Power spectrum estimates and autocorrelation of bandlimited PN (Case 2 of Table 1: **BW** = 150-250 Hz; Z = 2047 bits)

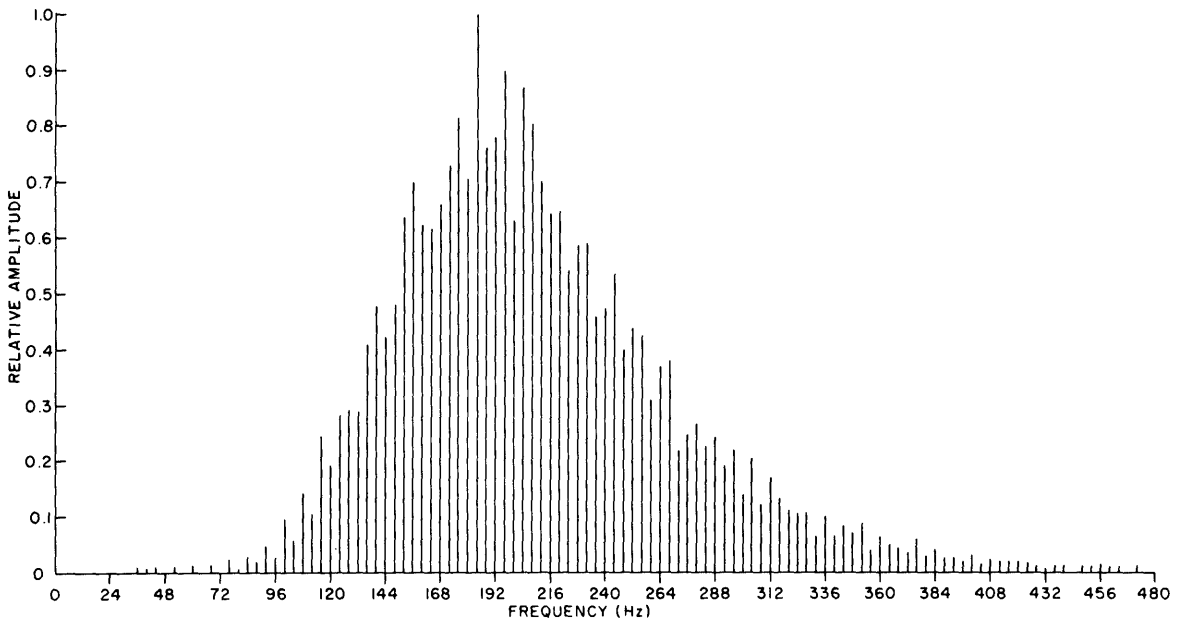

(a) Power spectrum

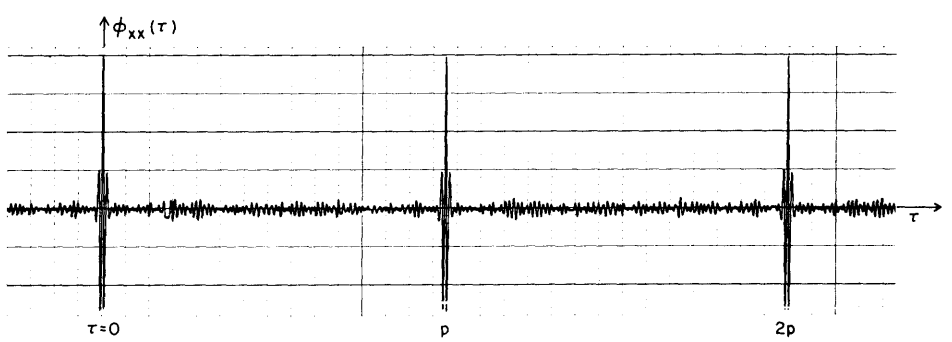

(b) Autocorrelation

Fig. 11 – Power spectrum estimates and autocorrelation of bandlimited PN (Case 3 of Table 1: BW = 150-250 Hz; Z = 4095 bits)

These few examples of power spectrum for the three selected PN sequences were introduced to see which sequence would be used as a reference model for future developments. Longer sequence lengths were not introduced because of the limitations imposed by the computer system being employed. The PN sequence of length $2^{10} - 1$ bits appears to be the one most suitable for our studies. We will call the power spectrum associated with that sequence the *signature* of the PN and any perturbations of this signal should reflect some changes in this *signature*.

Additive Noise Effect

The problem of noise in a communication system has been and will continue to be an area of concern to the communication engineer. The literature associated with and the methods of extracting signals from a noisy background has become a specialized area in engineering [11-13]. There is the classic study of shot noise due to thermionic emission of electrons in vacuum tubes [13] and the noise figure associated with amplifiers. In a communication system, noise is associated with the transmitter, antenna, transmission medium (air, water, or electric conductor), and receiver.

The problem of isolating the noise and finding the particular component associated with some particular component in the communication system is seldom undertaken [14]. Generally all the sources that contribute to the noise are considered in terms of their total effect or noise figure in the entire system. We are usually dealing with a system such that the signal-to-noise ratio will ultimately determine our success with a given situation.

This particular analysis will be concerned with the power spectrum of PN with additive noise. The noise component will be of the manufactured variety generated by a thermal noise source. This noise source is a Western Electric-Acoustic Laboratory type 300A, designed to furnish a broad, continuous, and steady noise spectrum. The fundamental source used in this instrument is the noise due to electronic agitation within a cold resistor. This arrangement is supposed to give a noise source that is extremely stable, being dependent only upon the magnitude of the resistor and the ambient temperature.

This fundamental noise source has a very low output and requires a large amount of amplification. Consequently, the electronic noise is amplified by a feedback amplifier providing about 100 dB gain. This noise source did not live up to the specifications set by the manufacturer, in that it was not stable and did not have a steady noise spectrum. Ideally we would have liked for the noise to have been *white* (constant power over the entire frequency spectrum).

The procedure in this experiment was to take some filtered PN and add to it various amounts of noise both wideband and narrow-band to obtain different signal-to-noise ratios and then compute the power spectrum along with the autocorrelation and also some cross-correlation. The purpose was to see what happens to the power spectrum of PN when it becomes deeply embedded in noise.

The recording setup was as shown in Fig. 12, and 26 recordings were made with this arrangement. A single PN sequence of length $2^{10} - 1$ bits and a sampling rate of 2000 Hz were used. A bandwidth of 100 Hz centered at 200 Hz was used for recording. The selection of the particular PN sequence to be used as well as the shift rate and sampling rate was based on previous considerations. The specifications associated with the PN are listed in Table 2.

The first 13 recordings were made using wideband noise and adding it linearly with the aid of an operational amplifier to the filtered PN (Fig. 12). The procedure was to set some voltage level as read by the rms meter with the thermal noise source disconnected. After establishing a level for the PN signal, this signal was disconnected and a reading was taken on the thermal noise source. The combined voltage value had to be such that it would not exceed full scale on the A/D converter. The corresponding voltage values were recorded, and their resulting signal-to-noise ratios were also recorded (Table 2).

Wideband noise was used on the signal to try to simulate a condition whereby one receives a bandlimited signal at a very low voltage level and employs a series of wide-band amplifiers to increase the level to some appropriate value. If a filter is not employed at the final output of these cascaded amplifiers, some wideband noise components could possibly be introduced on the signal.

The second set of recordings, 15 through 27, were made with the bandpass filter inserted after the noise source, and this filter had the same frequency response as that used with the PN signal. The procedure for adjusting the voltage levels was the same as for the first set explained earlier. In all cases, although not shown in Fig. 12, an isolation transformer was used between the wideband amplifier and A/D converter to keep out any dc bias.

The mathematical rationale associated with this noise analysis is straightforward and does not involve the more complex analysis of mean square error or threshold (detection) requirements. The filters used here are simply for bandlimiting purposes and do not perform any preprocessing such as smoothing or predicting and are not optimum filters or matched filters. The mathematical analysis for computing the power spectrum of a signal with additive noise can be handled by ordinary statistical methods.

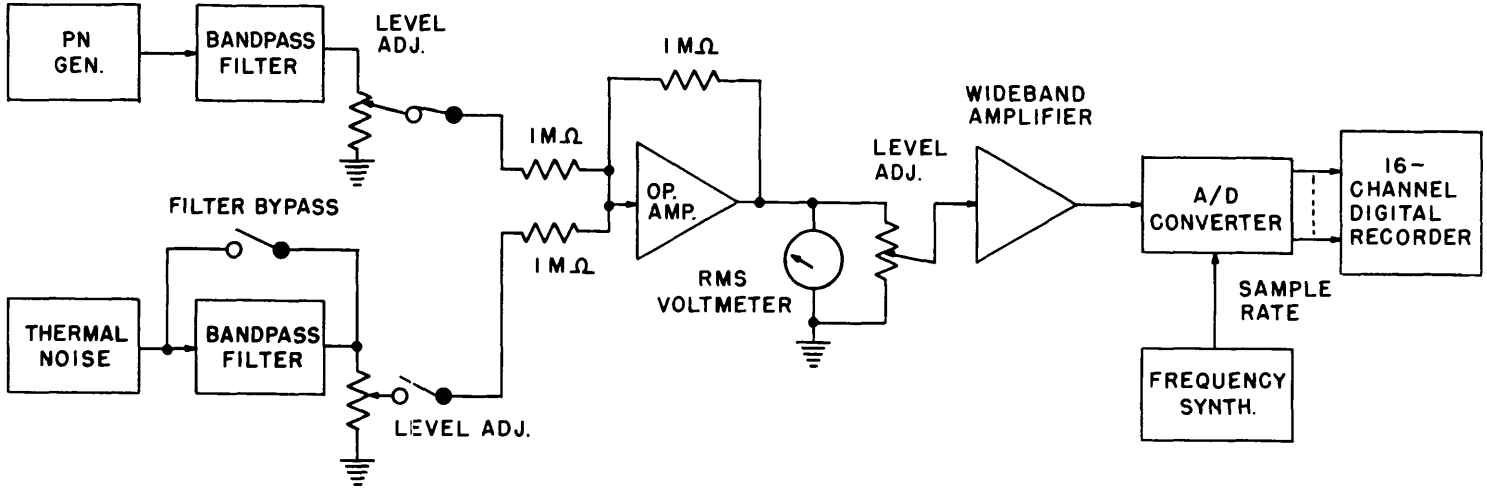

Fig. 12. – Digital recording of PN with additive noise.

We shall represent our periodic PN signal as $s(t)$ and let $n(t)$ be the additive noise without any periodic component. We further define a function $y(t)$ as being the sum of the two signals expressed as

$$y(t) = s(t) + n(t). \tag{25}$$

We will assume that signals can be treated as a *random process* (see Appendix C for definition of *italicized* terms). Both signals will have zero mean.

The autocorrelation function of $y(t)$ taken as an *ensemble average* is given by

$$\Phi_{yy}(\tau) = E\{[s(t) + n(t)]\,[s(t+\tau) + n(t+\tau)]\}. \tag{26}$$

If our process is *wide-sense stationary* the autocorrelation function is a function of the sample time interval τ, and since E is a linear operator we get the following, where a bar symbolizes ensemble average:

$$\Phi_{yy}(\tau) = \overline{[s(t)\,s(t+\tau)]} + \overline{[s(t)\,n(t+\tau)]} + \overline{[n(t)\,s(t+\tau)]} + \overline{[n(t)\,n(t+\tau)]}. \tag{27}$$

which gives us

$$\Phi_{yy}(\tau) = \Phi_{ss}(\tau) + \overline{[s(t)\,n(t+\tau)]} + \overline{[n(t)\,s(t+\tau)]} + \Phi_{nn}(\tau). \tag{28}$$

We further assume that $s(t)$ and $n(t)$ are *statistically independent*, which allows us to separate the second and third terms in Eq. 28 into

$$\overline{s(t)\,n(t+\tau)} = \overline{s(t)}\;\overline{n(t+\tau)} \tag{29a}$$

and

$$\overline{n(t)\,s(t+\tau)} = \overline{n(t)}\;\overline{s(t+\tau)}. \tag{29b}$$

But

$$\overline{s(t)} = \text{mean value of } s(t) \tag{30a}$$

and

$$\overline{n(t)} = \text{mean value of } n(t). \tag{30b}$$

From our previous assertion that both signals, $s(t)$ and $n(t)$ will have zero mean, Eqs. 29a and 29b will equal zero; therefore

$$\Phi_{yy}(\tau) = \Phi_{ss}(\tau) + \Phi_{nn}(\tau). \tag{31}$$

By application of the Wiener-Khintchine theorem, the power spectrum will be the Fourier transform of the autocorrelation function, giving

$$W_{yy}(f) = W_{ss}(f) + W_{nn}(f). \tag{32}$$

Equation 32 shows that our power spectrum will be simply the contributions of the power spectrum of the original signal added to the noise. If we were truly successful with the linear addition of noise to our signal, we should be able to subtract the power spectrum of our noise from our combined spectrum and be left with the spectral power of our signal.

The computed results for the power spectrum are shown in Figs. 13 through 18 and the data for the various cases are tabulated in Table 2. Included with plots of the power spectrum are the autocorrelations and, in some cases, the crosscorrelation between the reference PN without noise against the signal under investigation.

Figure 13a is the power spectrum of the wideband thermal noise source (Case 1 of Table 2). The spectrum is not constant over the frequency band and therefore cannot be considered as *white* noise. The autocorrelation function (Fig. 13b) shows no periodic components.

Figure 14 is Case 8, where the signal-to-noise ratio equaled zero. We can still see the envelope associated with the PN power spectrum (Fig. 14a) and the wideband additive noise filling in the background. The autocorrelation (Fig. 14b) is still well defined, indicating that a periodic signal is still present, but the peak values are less than half of what they were for the PN signal alone.

Figure 15 is Case 10, where the signal-to-noise ratio is now –10 dB. The power spectrum shows no evidence of the PN signal and has essentially the same appearance as the wideband noise in Fig. 13a. The autocorrelation (Fig. 15b) fails to show any periodic components, but the crosscorrelation of the reference PN signal against this noise corrupted signal (Fig. 15c) reveals a detectable periodic component. This shows that while there is nothing to be gleaned from the power spectrum or autocorrelation for this particular case of additive noise, there seems to be some processing gain associated with comparing a clean signal against one deeply embedded in noise.

The second half of this analysis deals with the same PN signal, but the additive noise has been filtered through the same type of filter as the PN. The data for these cases are in Table 2 (Cases 15 through 27). Figure 16a is the power spectrum for the bandlimited thermal noise and represents Case 15. The filtered noise shows very heavy components representing harmonics of 60 Hz. This becomes a good example of noise with a few transient spikes mixed in and represents a very undesirable situation in a communication system. The autocorrelation (Fig. 16b), although it does not indicate any cyclic components, has considerably higher values than that associated with the wideband noise of Fig. 13a; there appears to be a modulation effect on the autocorrelation.

Figure 17a is the spectral power associated with Case 22, where the S/N equals 0 dB. There is almost a complete deterioration of the PN power spectrum, and the

harmonics of 60 Hz are very pronounced. The gaps between the harmonic separation of the PN have been entirely filled in by the additive noise. There would be very little confidence associated with trying to identify the PN in this spectrum plot. The autocorrelation and the crosscorrelation (of Case 22 against Case 16) continue to give meaningful results (Figs. 17b and 17c). The crosscorrelation still gives higher values than the autocorrelation.

Figure 18a is the spectrum for a S/N ratio of –10 dB and represents Case 24. The power spectrum has been corrupted to the point of representing nothing more than the power spectrum of the bandlimited noise plotted in Fig. 16a. The plots of the autocorrelation (Fig. 18b) also fail to yield the periodic components associated with the PN. However, the crosscorrelation of the noise corrupted PN signal versus the reference PN (Case 16) continues to give noticeable peaks at each period of the PN (Fig. 18c).

The plots of the three remaining cases (not shown) fail to yield anything for power spectrum or correlations; they are essentually the point at which this type of analysis fails to give any meaningful results.

The attempt to subtract the power spectrum of the thermal noise from that of the combined signal plus noise fails to yield the power spectrum of the signal. Ideally (Eq. 32) we should be able to perform

$$\mathbf{W}_{ss}(f) = \mathbf{W}_{yy}(f) - \mathbf{W}_{nn}(f). \tag{33}$$

One reason Eq. 33 is not applicable in this analysis may be that the computer has normalized the values of the power spectrum, therefore making a linear subtraction all but meaningless. Another reason is that the crosstalk due to the frequency components associated with the noise spikes cannot be resolved. A final and probably the most important reason can be found in Eq. 27. We showed that the second and third terms of Eq. 27 vanished because s(t) and n(t) are *statistically independent*. However, in actual computation there is a crosscorrelation of low level associated with Fig. 15. This means that these two terms are not identically zero but have a significant value over the time duration that this analysis was being performed. This means that Eq. 27 will be transformed as follows:

$$\mathbf{W}_{yy}(f) = \mathbf{W}_{ss}(f) + \mathbf{W}_{sn}(f) + \mathbf{W}_{ns}(f) + \mathbf{W}_{nn}(f), \tag{34}$$

which indicates that we can no longer simply subtract $\mathbf{W}_{nn}(f)$ from $\mathbf{W}_{yy}(f)$ and get $\mathbf{W}_{ss}(f)$. However, if the other two components in Eq. 34 were included, all three terms could be subtracted from the additive noise spectrum, leaving the spectrum of the signal, provided we still adjust for the normalization effects.

Table 2

Cases Recorded for PN Sequences with Additive Noise
($Z = 2^{10} - 1 = 1023$ bits; Bandwidth = 150 to 250 Hz; Shift Rate = 8184 Hz)

Case	s(t) PN Signal (dB)	n(t) Noise Vol. (dB)	S/N Ratio (dB)	Δf Computer Program Resolution (Hz)	f Harmonic Separation (Hz)	X Sampling Rate (Hz)
Wideband Thermal Noise						
1	0	−10	−∞	4	8	2000
2	−3.5	0	+∞	"	"	"
3	−2	−27	+25	"	"	"
4	−2	−22	+20	"	"	"
5	−2	−17	+15	"	"	"
6	−2	−12	+10	"	"	"
7	−2	−7	+5	"	"	"
8	−2	−2	0	"	"	"
9	0	+5	−5	"	"	"
10	−5	+5	−10	"	"	"
11	−10	+5	−15	"	"	"
12	−15	+5	−20	"	"	"
13	−20	+5	−25	"	"	"
14*	–	–	–	–	–	–
Narrow-Band Thermal Noise (150 to 250 Hz)						
15	0	−8	−∞	4	8	2000
16	−5	0	+∞	"	"	"
17	0	−25	+25	"	"	"
18	0	−20	+20	"	"	"
19	0	−15	+15	"	"	"
20	0	−10	+10	"	"	"
21	−5	−10	+5	"	"	"
22	−10	−10	0	"	"	"
23	−15	−10	−5	"	"	"
24	−20	−10	−10	"	"	"
25	−25	−10	−15	"	"	"
26	−30	−10	−20	"	"	"
27	−35	−10	−25	"	"	"

*Not transferred to the IBM reel.

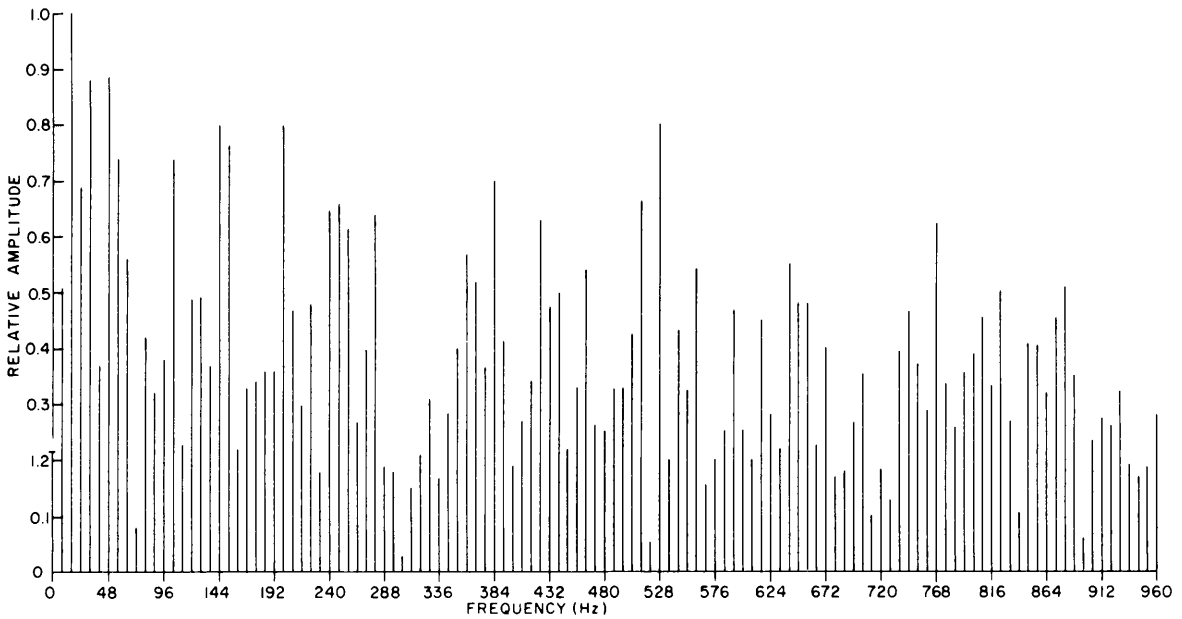

(a) Spectrum of wideband thermal noise

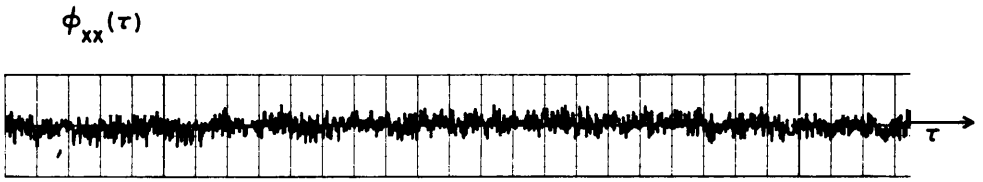

(b) Autocorrelation

Fig. 13 – Spectrum of wideband thermal noise (Case 1 of Table 2)

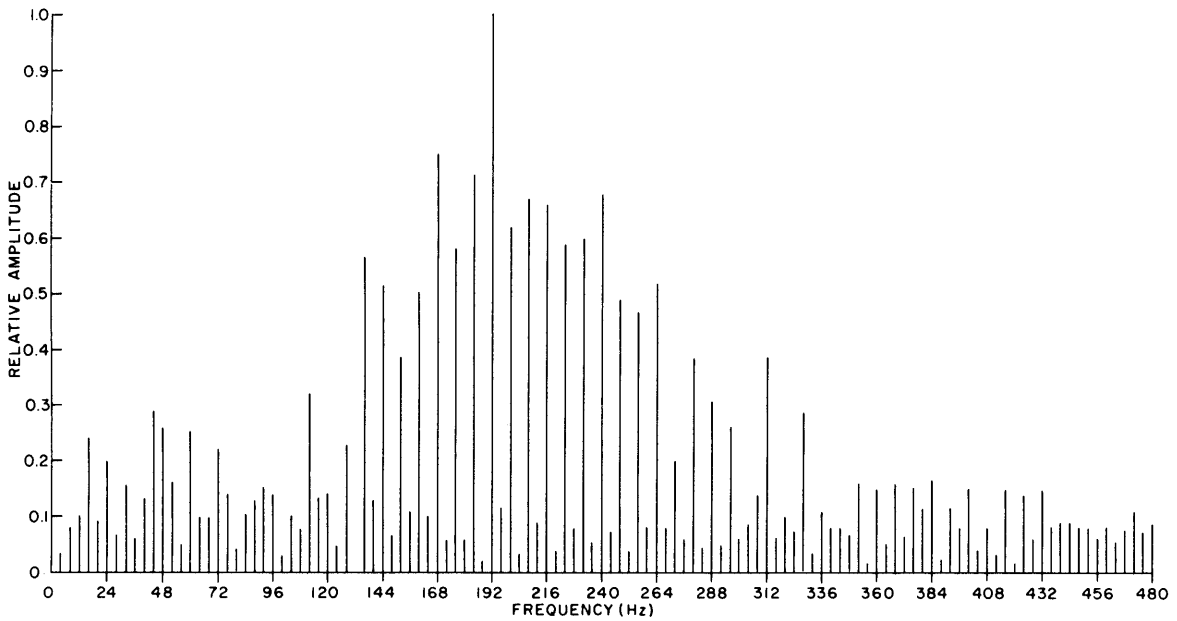

(a) Power spectrum

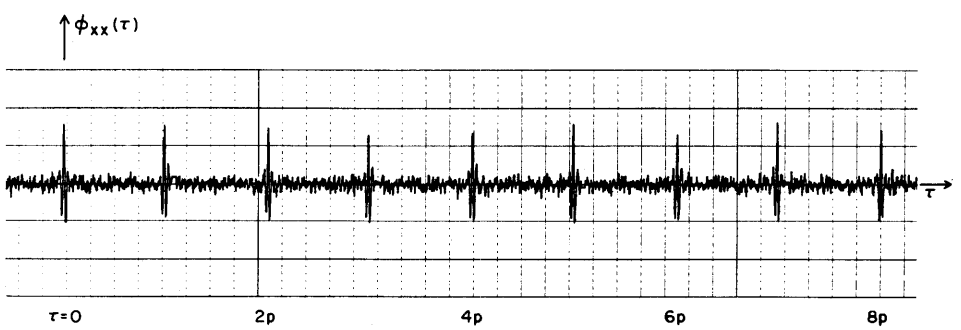

(b) Autocorrelation

Fig. 14 – Effects of additive wideband thermal noise on the bandlimited PN power spectrum and correlation (Case 8 of Table 2: S/N ratio = 0 dB)

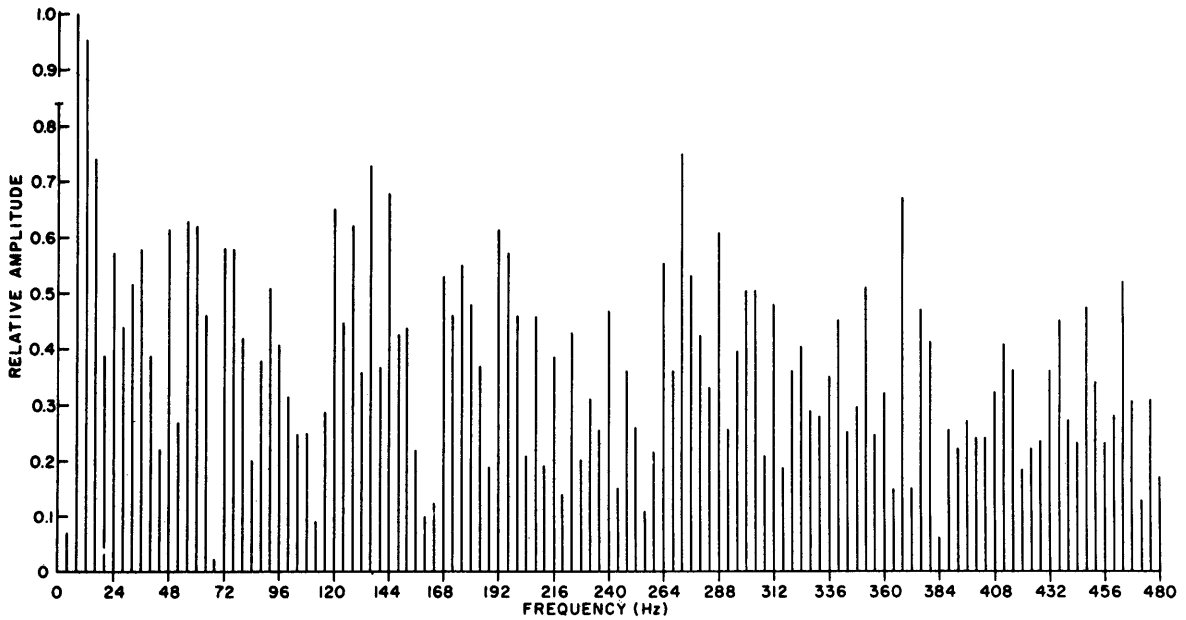

(a) Power spectrum

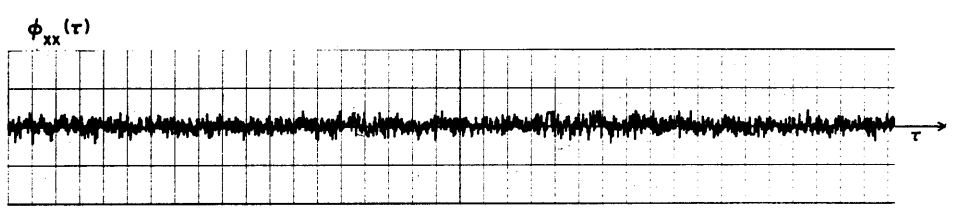

(b) Autocorrelation

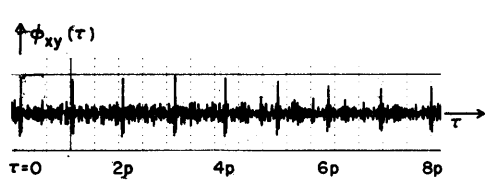

(c) Crosscorrelation of the reference PN signal and Case 10

Fig. 15 – Power spectrum and correlations of additive thermal noise and PN (Case 10 of Table 2: S/N ratio = –10 dB)

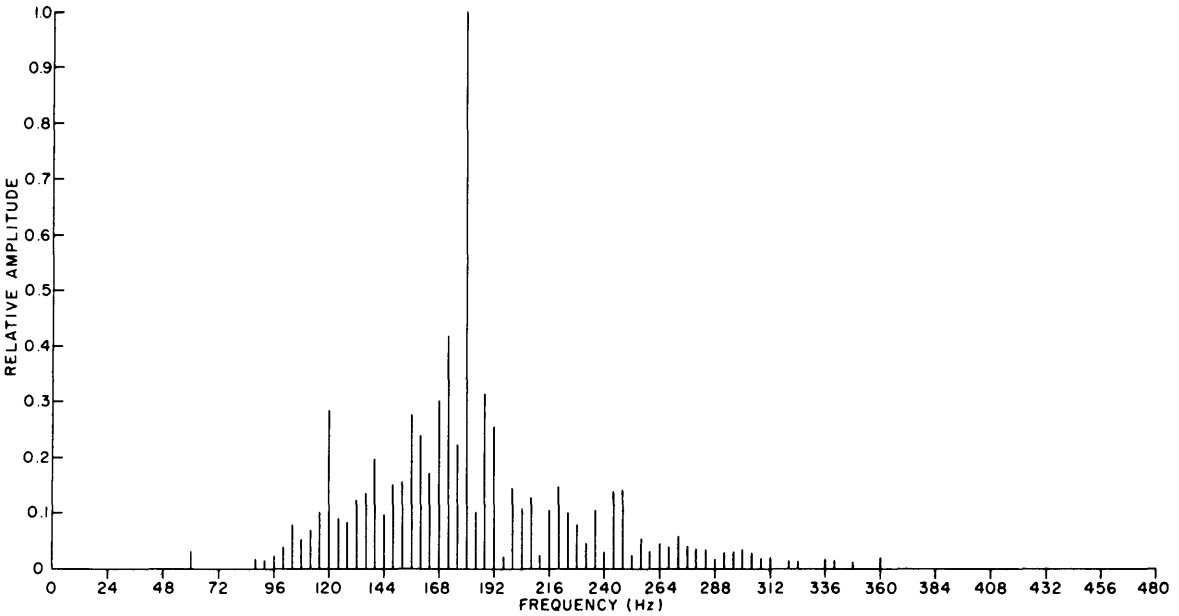

(a) Power spectrum

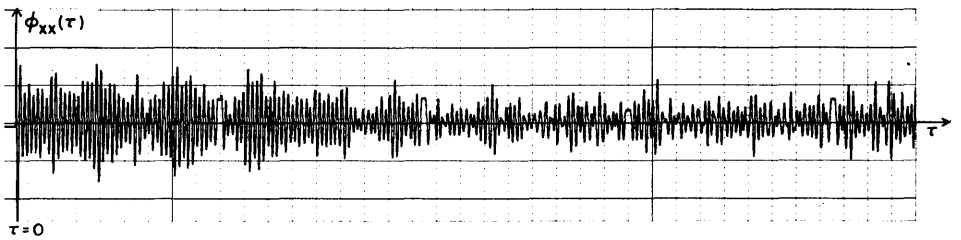

(b) Autocorrelation

Fig. 16 – Spectrum of narrowband thermal noise (Case 15 of Table 2: BW = 150-250 Hz)

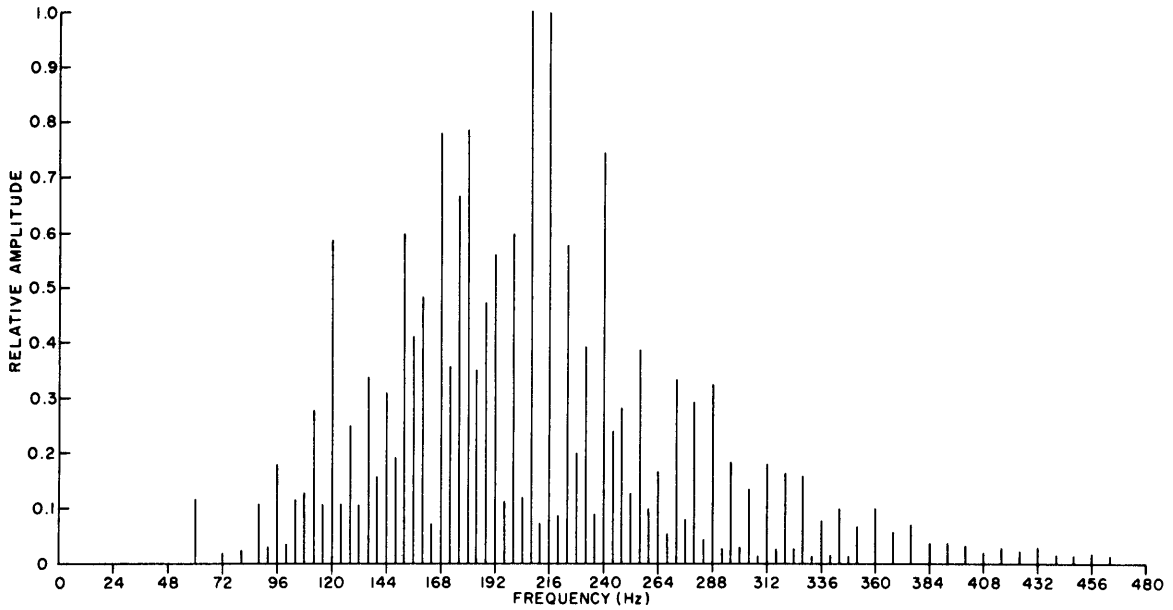

(a) Power spectrum

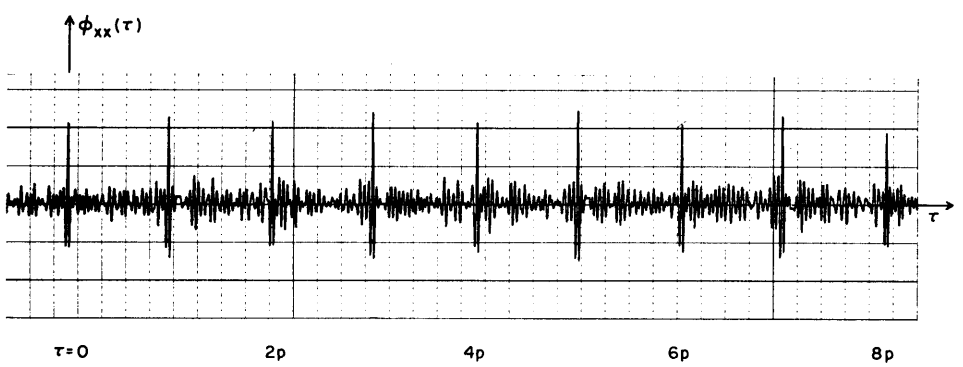

(b) Autocorrelation

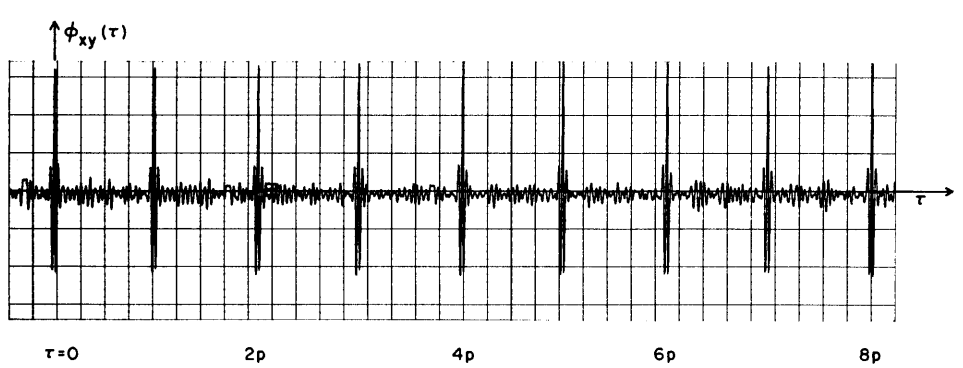

(c) Crosscorrelation of Case 16 (reference PN) against Case 22

Fig. 17 – Effects of additive thermal noise on PN power spectrum and correlations – both bandlimited (Case 22 of Table 2: BW = 150-250 Hz; S/N ratio = 0 dB)

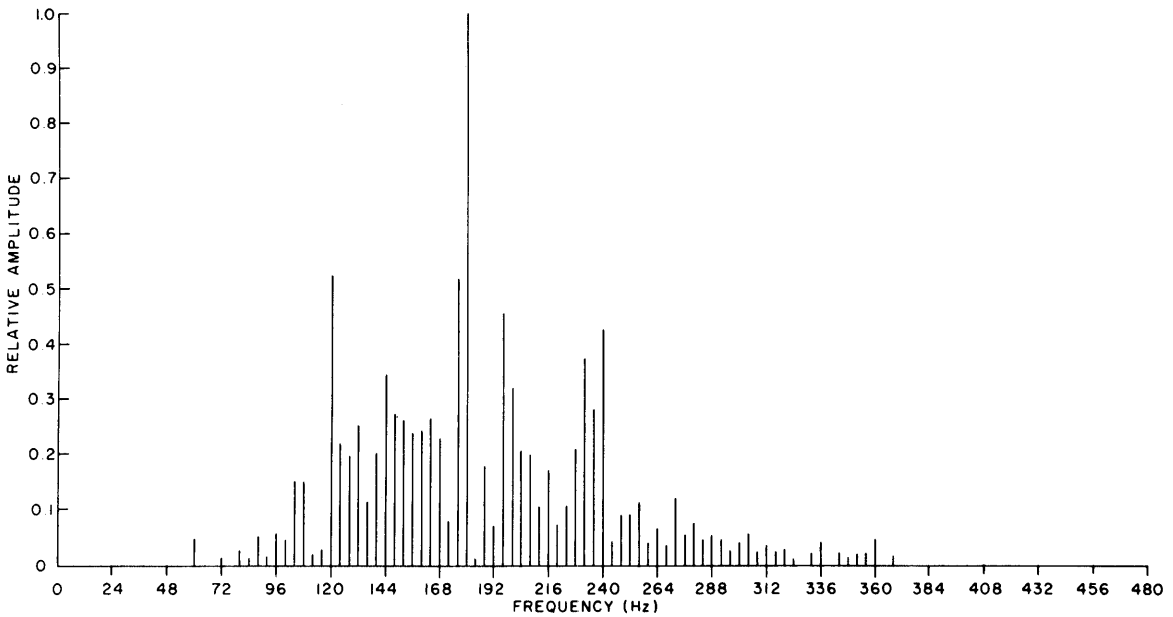

(a) Power spectrum

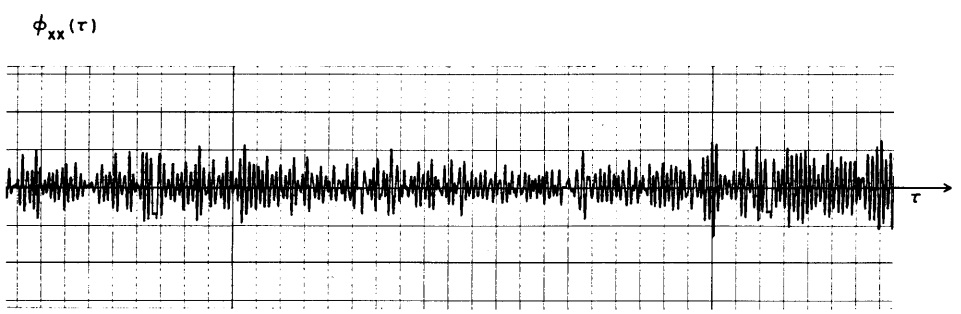

(b) Autocorrelation

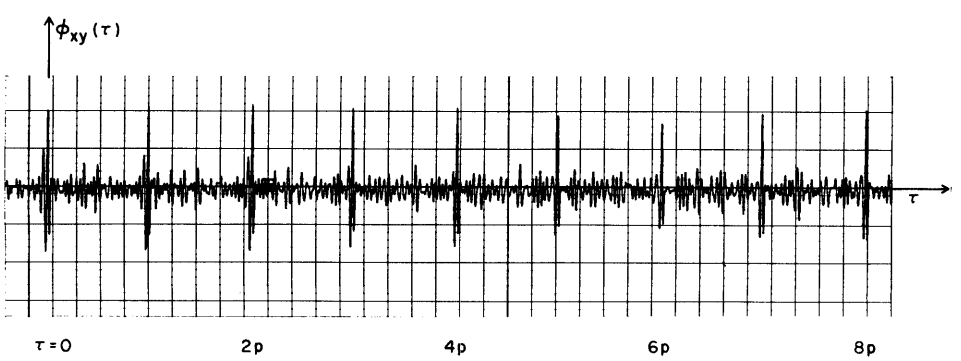

(c) Crosscorrelation of the Case 16 against Case 24

Fig. 18 – Effects of additive thermal noise on PN power spectrum and correlations – both bandlimited (Case 24 of Table 2: BW = 150-250 Hz; S/N ratio = −10 dB)

Multiple-Path Effect

In addition to the problem of additive noise on a signal, another phenomena associated with the reception of a transmitted signal is multiple path. Multiple path poses a problem to the communication engineer whether the transmitted signal is electromagnetic or acoustic. The result of this multiple path is the creation of a signal that consists of several signals overlapping one another. The resultant signal is sometimes referred to as a multiple-epoch signal [15], but more commonly in acoustics it is called simply a multipath signal [16].

The object of this phase of study is to see what effects multipath has on filtered PN and in particular what effect it has on the power spectrum of the PN. The PN selected for this analysis has a sequence length of 1023 bits and is shifted at 8184 bits per second. The multipath analysis will be concerned with the noiseless case only. A few cases of multipath will be considered and will consist of the original signal plus a single delayed replica overlapping it. The other cases of multipath will be the signal plus two delayed replicas (different amounts of delay) all overlapping.

A symbolic representation of the multipath effect is shown in Fig. 19. The recording procedure was essentially the same as that used for the additive noise study, with the insertion of a tapped delay line to simulate multipath effects. There were 12 cases recorded, all with a sampling rate of 2000 Hz. The specifications for the PN and bandwidths are listed in Table 3. The first six cases used a bandwidth of 100 Hz centered at 200 Hz, and the second six cases used a bandwidth of 300 Hz centered at 300 Hz. The tapped delay line had a maximum delay of 5 milliseconds (ms) and the PN period was 125 ms, so the maximum delay was 1/25th of the PN period. The delay line had 100 taps representing increments of 0.05 ms of delay. However, these very small increments of delay were so small compared to a PN period they proved to be ineffectual in the experiment, and only delays representing multiples of 1 ms were employed.

We can obtain the power spectrum of the multipath PN by employing essentially the same techniques used in the additive noise case. Let $s(t)$ represent our periodic PN signal and $s(t - kT)$ represent the delayed component, where T equals 1 ms and k takes on integer values of 1 through 5. The output signal $y(t)$, Fig. 19, can be written as

$$y(t) = \sum_{k=0}^{n} s(t - kT), \qquad n = 1, 2, 3, 4, 5. \tag{35}$$

We shall always be working with $s(t)$ plus the addition of one or more delayed replicas of $s(t)$; hence the general expression in Eq. 35 will not yield $s(t)$ alone.

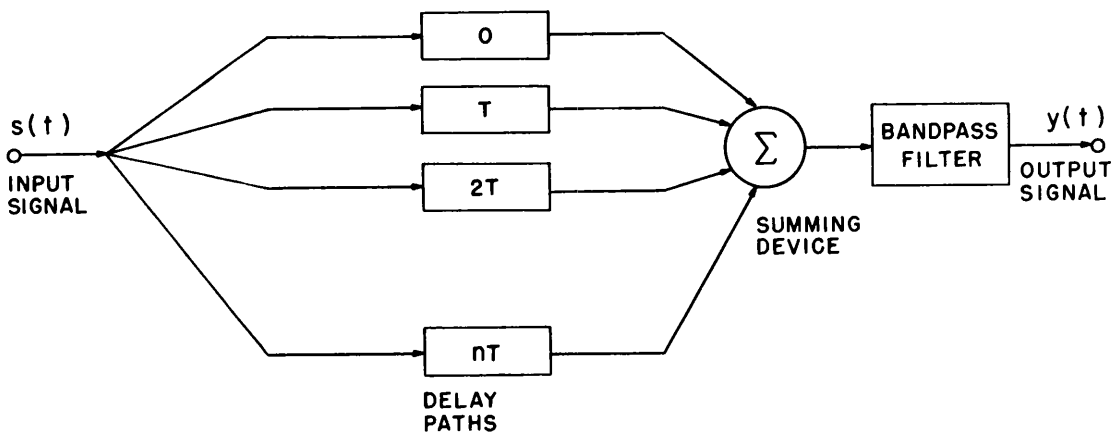

Fig. 19 – Multiple-path effects

Table 3

Cases Recorded for Effects of Multipath on PN Sequences

Case	n Shift Register Length	X Sample Rate (Hz)	Δf Computer Program Resolution (Hz)	f Harmonic Separation	f_s Shift Rate (Hz)	Bandwidth (Hz)	ΔT Delay (ms)
1	10	2000	4	8	8184	150-250	1
2	"	"	"	"	"	"	3
3	"	"	"	"	"	"	5
4	"	"	"	"	"	"	1,3
5	"	"	"	"	"	"	1,5
6	"	"	"	"	"	"	3,5
7	"	"	"	"	"	150-450	1
8	"	"	"	"	"	"	3
9	"	"	"	"	"	"	5
10	"	"	"	"	"	"	1,3
11	"	"	"	"	"	"	1,5
12	"	"	"	"	"	"	3,5

Assuming a wide-sense *stationary* process with zero mean, we can write the autocorrelation function of $y(t)$ as an *ensemble average* for the case where $n = 1$ in Eq. 35:

$$E[y(t)\,y(t+\tau)] = [s(t) + s(t-T)]\,[s(t+\tau) + s(t+\tau-T)]. \tag{36}$$

This gives us

$$\Phi_y(\tau) = 2\Phi_{ss}(\tau) + \Phi_{ss}(\tau - T) + \Phi_{ss}(\tau + T). \tag{37}$$

The Fourier transform of Eq. 37 will yield the power spectrum:

$$W_y(f) = 2W_{ss}(f) + W_{ss}(f)\,e^{-j2\pi fT} + W_{ss}(f)\,e^{j2\pi fT} = 2W_{ss}(f)(1 + \cos 2\pi fT). \tag{38}$$

It would appear at first glance that Eq. 38 can be extended for any single value of delay that is an integral multiple of T, but this is not the case. A modification of Eq. 37 will allow us to express the power spectrum for a single delay that is an integral multiple of T milliseconds. Extending Eq. 37 for this special case will give

$$W_y(f) = 2W_{ss}(f)(1 + \cos 2\pi mfT), \tag{39}$$

where m is any integer not equal to zero.

Equation 39 shows that the power spectrum for a single multipath signal is twice the spectrum of the undelayed signal plus twice the spectrum of the mth harmonic. At first glance it would appear that we are getting extra power from a signal that has broken off into multiple paths, but this is not the case. The power components associated with the cosine term can cause canceling effects for some of the frequencies, and in an extreme case the overall effect of the multipath signal can give rise to complete cancellation of power components associated with the fundamental frequency terms.

A general expression for the power spectrum using Eq. 35 can be readily obtained but will be deferred until later in this analysis. For the present we will develop the power spectrum for the various values of delay and combinations thereof that are used in this study. Our general expression obtained in Eq. 39 will take care of six of the cases in Table 3, where only one multipath was considered. For Cases 4 and 10 of Table 3, where two multipaths were considered with delays of 1 and 3 ms, our output signal $y(t)$ will take the form

$$y(t) = s(t) + s(t-T) + s(t-3T). \tag{40}$$

Using the same procedure as was used for the single multipath case, we can compute the power spectrum from the autocorrelation function and get

$$W_y(f) = W_{ss}(f)\,(3 + 2\cos 2\pi fT + 2\cos 4\pi fT + 2\cos 6\pi fT). \tag{41}$$

The same analysis can be extended for the other cases associated with Table 3 and obtain similar results as that given by Eq. 41, with the exception of the argument of the cosine terms. The total number of terms within the brackets of Eq. 41 will remain the same as well as the values of the constant terms (this is true for the special cases given in Table 3 and is not true in general, as will be seen in later developments). Table 3 reveals that the delay terms are not taken in sequence but involve only two delay terms at most, plus the undelayed signal $s(t)$.

To complete the analysis associated with the delays given in Table 3, we next consider Cases 5 and 11. From our general expression in Eq. 35, $y(t)$ will have the form

$$y(t) = \sum_{k=0}^{n} s(t - kT).$$

For $n = 5$ and $k \neq 2$, 3, or 4,

$$y(t) = s(t) + s(t - T) + s(t - 5T). \tag{42}$$

The power spectrum becomes

$$W_y(f) = W_{ss}(f)\,(3 + 2\cos 2\pi fT + 2\cos 8\pi fT + 2\cos 10\pi fT). \tag{43}$$

The power spectrum for Cases 6 and 12 can also be obtained by first noting that

$$y(t) = s(t) + s(t - 3T) + s(t - 5T), \tag{44}$$

and from this the spectrum will become

$$W_y(f) = W_{ss}(f)\,(3 + 2\cos 4\pi fT + 2\cos 6\pi fT + 2\cos 10\pi fT). \tag{45}$$

Thus far the expressions for the power spectrum for all 12 cases have been considered and it appears that a pattern is being formed so that we can obtain a general expression for the power spectrum for the number of multipaths considered and the amount of delay associated with each path. We shall defer the development of this general expression until after the results of the data have been analyzed.

The item of interest here is that for any delay path, or combinations thereof, that are integer multiples of some given delay T the power spectrum contains cosine terms that are all even harmonics. The extent of these harmonics will be better understood in later developments.

Returning our attention to the data associated with Table 3, we find some interesting developments. Figures 20 and 21 are for Cases 3 and 9 respectively. The bandwidths are 150 to 250 Hz and 150 to 450 Hz and the multipath delay is 5 ms. The

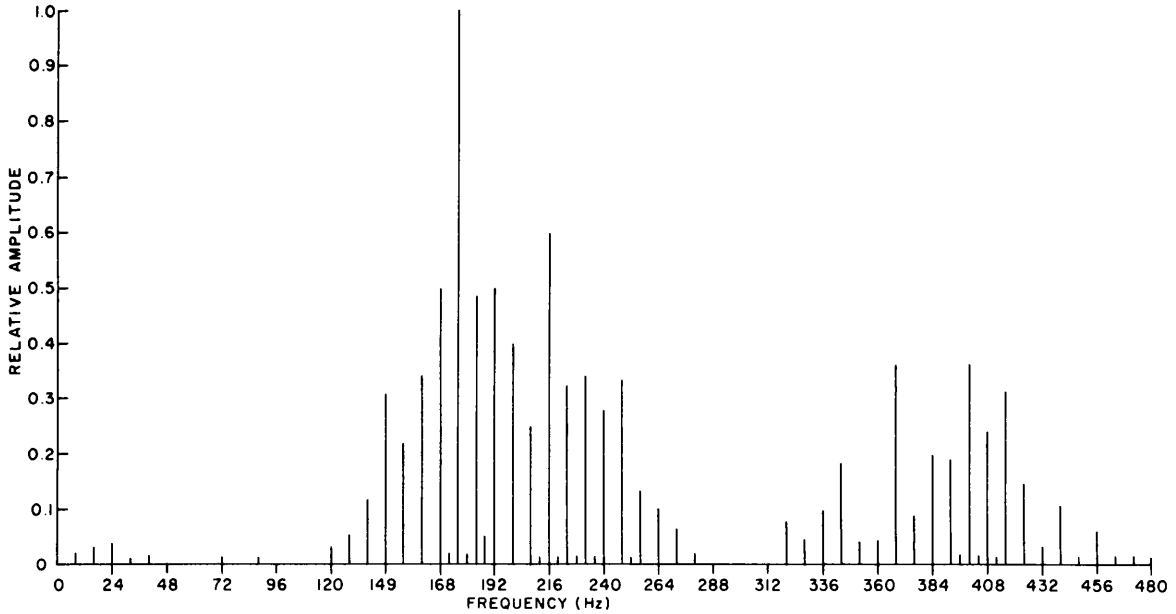

(a) Power spectrum

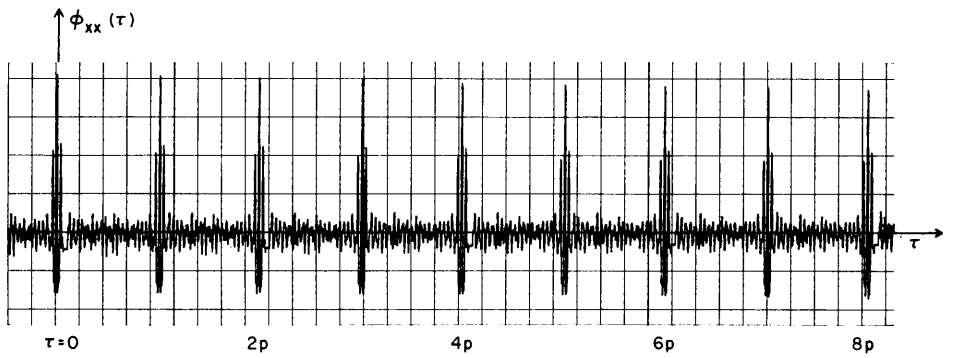

(b) Autocorrelation

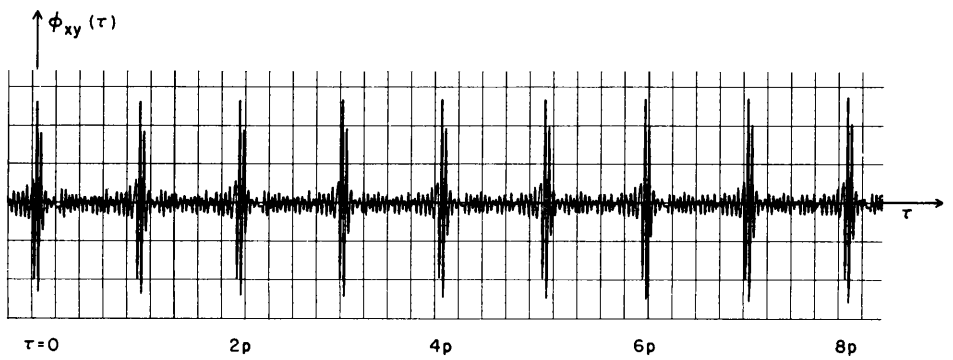

(c) Crosscorrelation of the reference PN against Case 3

Fig. 20 – Effects of single multipath on PN power spectrum and correlations (Case 3 of Table 3: BW = 150-250 Hz; multipath = 5 ms)

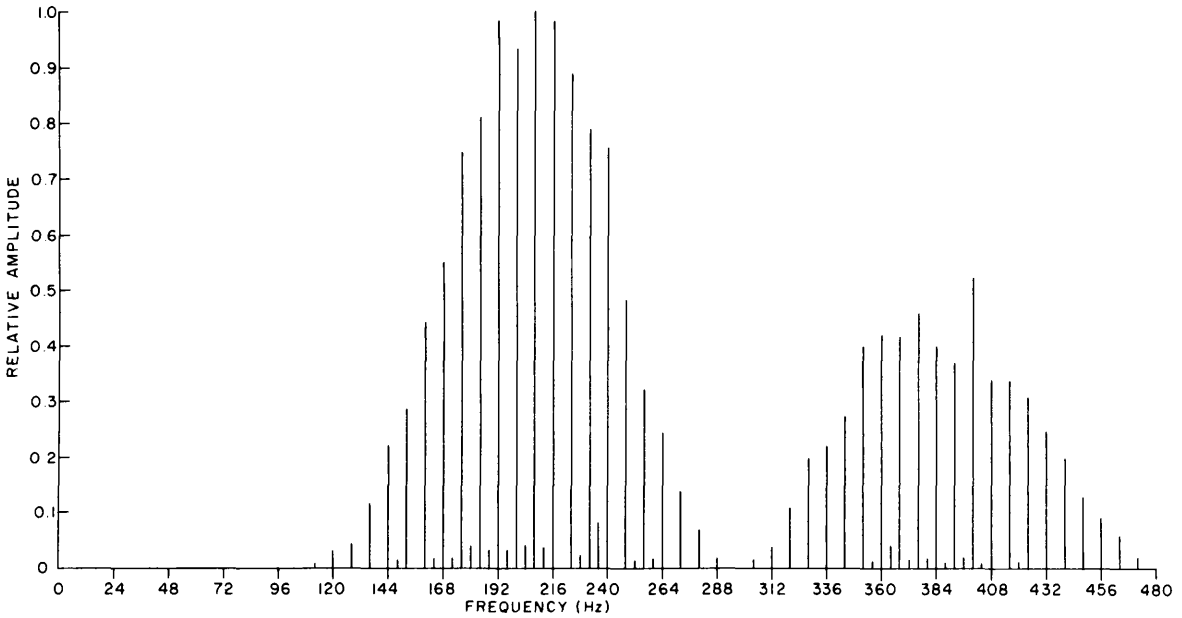

(a) Power spectrum

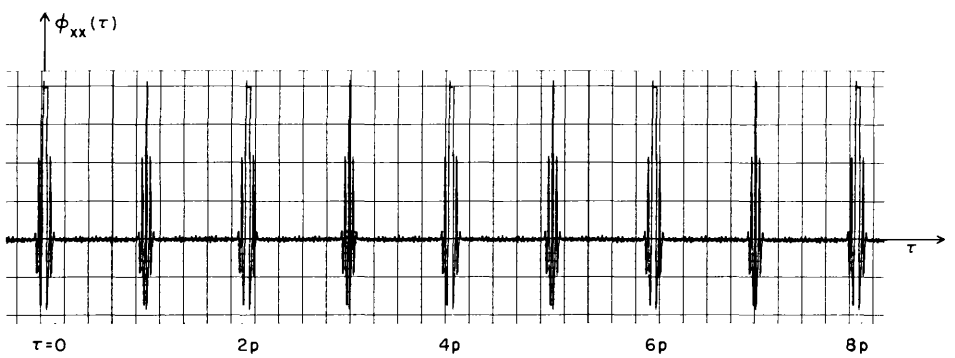

(b) Autocorrelation

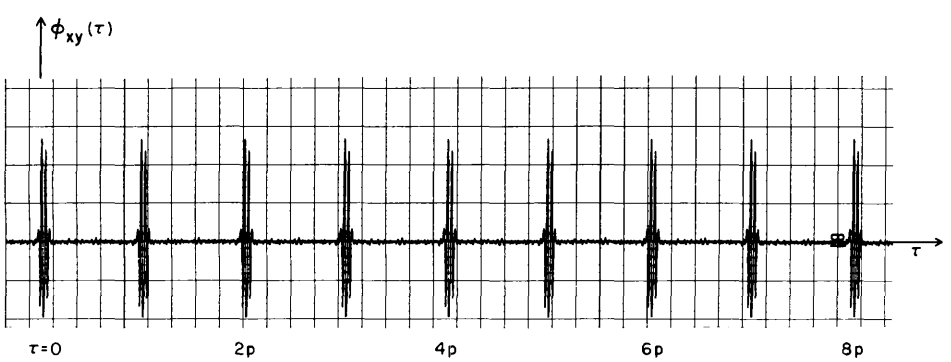

(c) Crosscorrelation of the reference PN against Case 9

Fig. 21 – Effects of single multipath on PN power spectrum and correlations (Case 9 of Table 3: BW = 150-450 Hz, multipath = 5 ms)

autocorrelations and crosscorrelations are presented with each plot of the power spectrum under consideration. The crosscorrelation is $s(t)$ versus the multipath signal of the same bandwidth. The correlations are shown without comment, since there does not appear to be anything unusual about them, and they are presented for purpose of comparison against the power spectrum.

Figure 21 represents the same value of multipath as Fig. 20 but a different bandwidth. The wider bandwidth of Fig. 21 shows how the power components are distributed. Notice the sizable secondary spectrum from 300 to 470 Hz. This secondary spectrum is well outside the band of Fig. 20 but has enough energy associated with it so as to be clearly visible. The two plots of Figs. 20 and 21 correspond to Eq. 39 with $m = 5$. The effects of this single cosine term has a marked effect on the power spectrum, where components of frequency are either reinforcing the fundamental or canceling it out.

In all cases of multipath considered, the envelope of the power spectrum was governed by the modulating effects of the cosine terms. The reinforcing of power components at various values of frequency were so strong that very significant power terms were displayed well outside the narrow band of 150 to 250 Hz. The wider band gave a better representation of the power distribution for the cases considered.

Had we been able to incorporate delays that represented a more significant percentage of the PN period, the effects of power spectrum as well as the correlation would have been more dramatic. Specifically, the larger values for the delay path would have reduced the power components within our band considerably. Since multipath represents a form of interference with the original signal, the effects of this interference has to be reflected somewhere in the spectral analysis. These longer delay paths would put power at harmonic frequencies that are considerably outside our passband and consequently subtract from the power within the band.

The correlation analysis would reveal these multiple returns as secondary peaks, well removed from the peak at $\tau = 0$. In actual practice, by crosscorrelating the received multipath signal with a reference signal, the measurement of the distance of the secondary peaks from that of the main peak will give an indication of length of the delay path or paths.

We should like to complete our analysis of multipath effects by computing a general expression for the power spectrum from the general expression of Eq. 35. If we change the indexing in Eq. 35 to $n - 1$ instead of n, we get

$$y(t) = s(t) + s(t - T) + s(t - 2T) + \ldots + s[t - (n - 1)T]. \tag{46}$$

If we take the Fourier transform of Eq. 46, we get

$$Y(f) = S(f) + S(f)\, e^{-j2\pi fT} + S(f)\, e^{-j4\pi fT} + \ldots + S(f)\, e^{-j2\pi fT(n-1)}$$

$$= S(f)\, [1 + e^{-j2\pi fT} + (e^{-j2\pi fT})^2 + \ldots + (e^{-j2\pi fT})^{n-1}]. \tag{47a}$$

Since the geometric progression is of the form

$$S = a + ar + ar^2 + \ldots + ar^{n-1} = a\left(\frac{1 - r^n}{1 - r}\right)$$

Eq. 47a can be written as

$$Y(f) = S(f)\left(\frac{1 - e^{-j2\pi fnT}}{1 - e^{-j2\pi fT}}\right)$$

$$= S(f)\, e^{j\pi fT(n-1)}\left(\frac{\sin \pi fnT}{\sin \pi fT}\right). \tag{47b}$$

The energy spectral density can be obtained from the relationship

$$W_y(f) = |Y(f)|^2, \tag{48}$$

and by noting that $|e^{j\pi fT(n-1)}|^2 = 1$, we get the expression

$$W_y(f) = W_s(f)\left(\frac{\sin \pi nfT}{\sin \pi fT}\right)^2, \tag{49a}$$

or by application of the Woodward [17] notation, where

$$\text{sinc } f = \frac{\sin \pi f}{\pi f}, \tag{49b}$$

Eq. 49a can be written in the form

$$W_y(f) = n^2 W_s(f)\left(\frac{\text{sinc } nfT}{\text{sinc } fT}\right)^2. \tag{49c}$$

Equations 49a and 49c are expressions for the power spectrum associated with the nongeneral expression given by Eq. 46. The reason Eqs. 46 and 35 are not general expressions for a multipath signal is that they only allow for a signal with successive increments of delay. Neither expression allows for arbitrary amounts of delay in the multipath structure; hence, the corresponding expressions for the power spectrum are not truly general.

A completely general expression for the power spectrum for any type of multipath signal can be obtained. Notice of the form that Eqs. 39, 41, 43, and 45 took for the various values of multipath considered leads to a general expression of the form*

$$W_y(f) = W_s(f) \left(m + 2 \sum_{\text{all}\,\Delta k} m_{\Delta k} \cos 2\pi \Delta k f T \right), \tag{50}$$

where m is the total number of k_i terms, $i = 0, 1, 2, \ldots, m-1$ and where k_i is some value of delay such that in the general expression for the multipath signal

$$y(t) = \sum_{i=0}^{m-1} s(t - k_i T) \tag{51}$$

$k_i T$ is the total amount of delay time for a given path and T is some convenient unit of time (1 minute, 1 second, etc.). Further, we define a parameter $\Delta k = |k_i - k_j|$, $i \neq j$, and define $m_{\Delta k}$ as the number of times a given value Δk appears.

A simple example will clarify the use of Eq. 50. We shall derive Eq. 41, which is the power spectrum for the multipath signal in Eq. 40 repeated here:

$$y(t) = s(t) + s(t - T) + s(t - 3T). \tag{40}$$

To apply Eq. 50 we see that there are three terms in Eq. 40; so $m = 3$. We have $k_i = 0$, 1, 3. Our difference terms are $\Delta k = 1, 2, 3$ respectively, with $m_{\Delta k} = 1$ for each Δk. Inserting the appropriate values in Eq. 50 gives

$$W_y(f) = W_s(f)\,(3 + 2 \cos 2\pi f T + 2 \cos 4\pi f T + 2 \cos 6\pi f T), \tag{52}$$

and we see that Eq. 52 is the same result as obtained in Eq. 41.

Correspondingly we can derive the power spectrum for the other cases of multipath that were considered in this report. We further assert that by application of Eq. 50 we can derive the power spectrum for any multipath signal, when the amount of delay time is known. For the cases when the delay paths appear in progressive numerical values Eq. 49a or 49c can be used as well as Eq. 50, which can always be used. Equation 49a can be transformed into the form of Eq. 50 by application of trigonometric identities, so that the sine term in the denominator can be divided out and the final expression transformed to cosine terms to correspond to Eq. 50.

*Equation 50 is a theoretical derivation by the author and coworker D. A. Swick of the Acoustics Division, Naval Research Laboratory.

Doppler Effect

Our last investigation on power spectrum of PN sequences will deal with the Doppler effect. The Doppler effect is the change in the apparent time interval between two events at a source which arises from the change in distance between the source and an observer together with the finite velocity of transmission of information about the events [18, 19]. The relative motion between a sound source and the observer along the line joining them causes a change in pitch as heard by the observer. The Doppler effect is not restricted to sound waves, but can act on any transmitted wave whether it be electromagnetic or acoustic waves. If there is no relative motion between source and observer, there is no Doppler effect.

The Doppler effect is one of the more common phenomena associated with sonar systems. The popular designation for the increase in pitch or frequency due to motion is called *up* Doppler; conversely for a decrease in pitch the effect is called *down* Doppler. The Doppler effect can also be considered as frequency compression or expansion. We shall develop the various cases of the Doppler effect and then apply them to some sampled data for power spectrum estimates.

Source in Motion – Referring to Fig. 22a we can calculate the Doppler effect for the source in motion toward a fixed observer. Velocities will be assumed constant and radial. The following notations will be used: c = velocity of sound (ft/sec), v_s = velocity of source (ft/sec), f = frequency of source (Hz), and SO = radial distance sound travels in 1 sec.

When there is no motion of source or receiver the f waves produced by the source S would travel the distance SO in 1 sec. When the source is moving toward the stationary observer O with velocity v_s, the f waves are now crowded into the space S′O in 1 sec, where $S'O = c - v_s$. The wavelength of the sound will be shortened from $\lambda = c/f$ to $\lambda' = (c - v_s)/f$ and the pitch $f' = c/\lambda'$ of the sound heard is

$$f' = f\,\frac{c}{c - v_s}. \tag{53}$$

If the source is receding, the sign of v_s is negative, so that the pitch f'' of the sound heard is

$$f'' = f\,\frac{c}{c + |v_s|}. \tag{54}$$

Observer in Motion – When the observer is moving with velocity v_o toward the stationary source (Fig. 22b), there is no crowding of waves, but the ear receives each

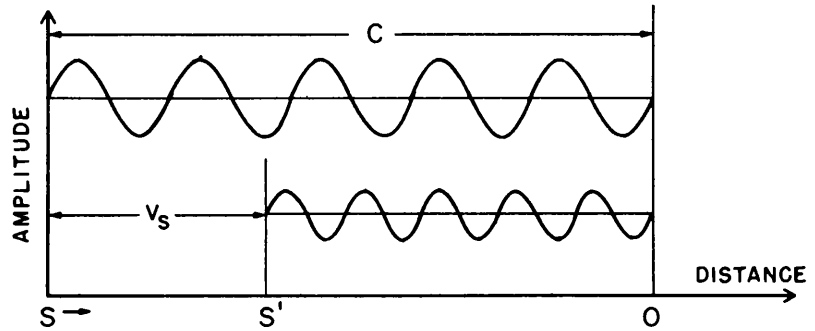

(a) f waves crowded into space $c - v_s$

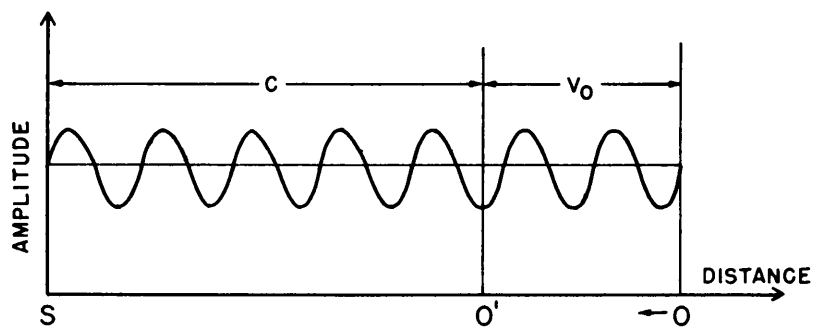

(b) Observer receives waves in space $c + v_o$ each second

Fig. 22 – Doppler effect

second not only the f waves in the interval c but an additional number v_o/λ in the distance $OO' = v_o$. Therefore, the increase in frequency heard is $f(v_o/c)$, and the pitch f' of the sound heard is

$$f' = f\left(1 + \frac{v_o}{c}\right). \tag{55}$$

If the observer is moving with velocity v_o away from a stationary source, the sign of v_o is negative, so that

$$f'' = f\left(1 - \frac{|v_o|}{c}\right). \tag{56}$$

In the two cases thus far considered, there is a definite physical difference between source or observation in motion. When the source is in motion the character of the waves is altered by a real change of wavelength. When the observer is in motion the wavelength is unchanged, but there is an apparent change of frequency due to his motion.

Source and Observer in Motion – By substitution of the results obtained in the preceding cases, one can obtain the Doppler effect for any combination of source and

observer in motion either toward or away or some combination thereof. For the case when source and observer approach each other, we get by substituting f′ of Eq. 52 for f in Eq. 55 a new f′ with the relationship

$$f' = f\left(\frac{c + v_o}{c - v_s}\right), \tag{57}$$

and for the case when source and observer recede from each other

$$f'' = f\left(\frac{c - |v_o|}{c + |v_s|}\right). \tag{58}$$

Equations 53 and 55 are the basic equations for the Doppler effect when either source or receiver respectively are in motion. Equation 57 is the basic equation for both source and receiver in motion. All three equations are applicable for any radial direction of velocity, and care must be exercised for the proper notation of sign (plus or minus) to be applied to the velocity terms in a given equation.

The terms in parenthesis in Eqs. 53 through 58 are sometimes referred to as the *Doppler stretch factor,* and implicit in this term *stretch* can be an increase or decrease in frequency depending on the direction (sign) of velocity. For a single frequency the Doppler effect can be considered as a frequency shift, causing either an increase or decrease in the frequency. However, in the case of a band of frequencies this frequency shift is different for each individual frequency component. The *Doppler stretch factor* is a constant for a given velocity of either source or observer, but when this constant value multiplies each frequency component in a band, the frequency shift will be proportional to the *un-Dopplered* value. For a given *Doppler stretch factor*, designated k the *Dopplered* bandwidth is given by

$$f_2' - f_1' = k(f_2 - f_1), \tag{59}$$

where f_1 and f_2 are the upper and lower frequencies in the band and k is determined by the appropriate terms in parenthesis in Eqs. 53 through 58.

We shall consider a method of introducing the Doppler effect in sampled data for the case where the observer is fixed and the source is in motion. Rather than assume some velocity of the source and from that calculate the Doppler component, we shall instead assume various values for the Doppler component and calculate the sampling rate needed to introduce this frequency change in an un-Dopplered signal. Since we are interested only in the Doppler effects on sampled PN sequences, we will not be concerned with the source velocities which would introduce these various Doppler values.

The test shall involve introducing a Doppler component in increments of 0.4 Hz until a maximum of ±3 Hz has been achieved. This will allow an analysis for both *up* and *down* Doppler or frequency expansion and compression for a bandwidth of 150 to 250 Hz.

Let the un-Dopplered signal have a sampling rate SR = 2000 samples per second, and let f_i be any frequency component in the band. The Doppler shift for any component frequency is then $f_i' - f_i = \Delta F$ and is either positive or negative depending on whether the Doppler shift is up or down.

We further notice that for an un-Dopplered signal and a given sampling rate there would be SR/f_i samples per cycle. If we consider the case of *up* Doppler, a given frequency component f_i would be shifted to a new value f_i' and

$$\frac{SR}{f_i} > \frac{SR}{f_i'}, \quad i = 1, 2, \ldots, m.$$

The Doppler effect can be simulated by changing our sampling rate to SR' such that $SR'/f_i = SR/f_i'$. Substituting $f_i' = kf_i$ we get

$$SR' = SR/k. \tag{60}$$

Since k is a constant, our new sampling rate SR' given by Eq. 60 is valid for any frequency f_i within the band.

Since the center frequency of our band is 200 Hz, we shall designate f_i equal to 200 Hz, and our ΔF will be associated with the Doppler shift for this frequency only. However, the ratio $\Delta F/f_i = k - 1$ is a constant for all frequency components within the bandwidth; therefore no additional errors are introduced by performing our calculations on the center frequency. Table 4 shows the tabulation for each assumed value of ΔF and the associated sampling rates calculated by Eq. 60 to give our simulated Doppler, where SR remained fixed and equal to 2000 Hz.

There were 19 recordings made on Dopplered PN sequences that had been filtered through a 150 to 250 Hz bandpass filter. The sequence length of the PN was 1023 bits and the shift rate was constant for the 19 cases at 8184 Hz. The recordings are tabulated in Table 4 and consist of one reference PN *un-Dopplered*, nine cases of *up* Doppler and nine cases of *down* Doppler, where the Doppler effect was changed by increments of $\Delta F = 0.4$ Hz.

Before viewing the results of the power spectrum estimates, some additional information would be instructive. Recall that Eq. 23 for power spectrum estimates was used to compute the power spectrum for all the PN studies thus far considered. It was also mentioned at that point, but not stressed, that Eq. 23 generated the *raw estimates* of spectral power that are computed for harmonics of Δf (program frequency resolution).

Table 4

Cases Recorded of the Effects of Doppler on PN Sequences

Case	ΔF Doppler Frequency Component (Hz)	Bandwidth (Hz)	X Sampling Rate (Hz)	Δf Computer Program Resolution (Hz)	f_0 Center Frequency (Hz)
1	0	150-250	2000	4.0	200
2	0.4	"	1996	3.992	"
3	0.8	"	1992	3.984	"
4	1.0	"	1990	3.980	"
5	1.4	"	1986	3.972	"
6	1.8	"	1982	3.964	"
7	2.0	"	1980	3.96	"
8	2.4	"	1976	3.952	"
9	2.8	"	1972	3.944	"
10	3.0	"	1970	3.940	"
11	−0.4	"	2004	4.0080	"
12	−0.8	"	2008	4.016	"
13	−1.0	"	2010	4.02	"
14	−1.4	"	2014	4.028	"
15	−1.8	"	2018	4.036	"
16	−2.0	"	2020	4.04	"
17	−2.4	"	2024	4.048	"
18	−2.8	"	2028	4.056	"
19	−3.0	"	2030	4.060	"

This calculation of the raw estimates is considered as being unsmoothed. The usual procedure is to calculate the smooth estimate of the power spectral density. The smoothing is a method of averaging over frequency to get truer estimates of power in the *neighborhood* of the frequencies being analyzed [1, 6, 10]. The technique of frequency smoothing is generally the *Hanning* method [1, p. 14].

The procedure for smoothing requires that we calculate an $S'_\tau(f)$ from the $S_\tau(f)$ where the prime indicates smoothing and no prime indicates the raw estimates. For $\tau = 0, 1, 2, \ldots, m$, we obtain

$$S'_0(f) = 0.5\ S_0(f) + 0.5\ S_1(f)$$

$$S'_\tau(f) = 0.25\ S_{\tau-1}(f) + 0.5\ S_\tau(f) + 0.25\ S_{\tau+1}(f),\ \tau = 1, 2, \ldots, m-1; \qquad (61)$$

$$S'_m(f) = 0.5\ S_{m-1}(f) + 0.5\ S_m(f).$$

Smoothing is necessary since the periodogram (raw estimate) given by Eq. 23 is considered an inefficient estimate of the true spectral density. The variability of these estimates does not decrease with increased record length or sample size. This leads to the requirement of smoothing the periodogram or, equivalently, weighing the correlation function nonuniformly. The rationale for weighing the correlation function stems from the fact it too is an estimate, and certain instabilities can occur that are reflected in the power spectrum; hence the need for smoothing.

The obvious question at this point would be, why the concern for smoothing now when in all our previous cases of analysis it was not used? The answer is that smoothing will always help the power spectrum estimates and will make the spectrum conform to some reasonable bounds. Our estimates prior to this Dopplered data did not appear to have any unusual appearances from what was anticipated. A few records were compared with their smoothed values and the change was not significant enough to incorporate smoothing throughout.

The power spectrum estimates of the Dopplered PN has dramatized the effects of smoothing; hence this technique was now introduced. Since PN has a power spectrum composed of discrete line frequencies, the Doppler effect would only serve to shift these frequency components by some amount ΔF, with the value of ΔF different for each individual frequency. The tabulated values of Δf (computer program resolution) are given in Table 4 for all the cases of the Doppler effect considered; they tend to indicate that the frequency shift would be too small to reflect any changes in the plots of the power spectrum.

Intuitively, one could assume that because all frequency components within a given band are shifted in proportion to the Doppler stretch factor, the net result of plotting all the various cases of Doppler considered in this report should have displayed essentially the same pattern of power spectrum. An examination of various cases of Doppler effect will reveal essentially the same power spectrum when smoothing was applied but a dramatic change on the plots of the unsmoothed spectrum.

Referring to Table 4, since Case 1 was the un-Dopplered data, it had the same spectrum as shown in Fig. 10a and is therefore not repeated in this presentation. Figure 23 is the spectrum for a frequency shift of 0.4 Hz associated with the center frequency and represents Case 2. Figure 23a is the smoothed spectrum and has a higher density of

spectral lines due to the smoothing routine. The appearance of the power spectrum conforms reasonably well with the frequency response of the bandpass filter. Figure 23b has the basic shape and density of the un-Dopplered PN, with the addition of small values of power components associated with frequencies within the band and extending well outside the bandpass region. The plots of the autocorrelation and crosscorrelation (Figs. 23c and 23d) show no significant changes for the amount of Doppler effect thus far considered.

Figure 24 represents the spectral plot for Case 6 in Table 4. The Doppler shift was $\Delta \mathbf{F} = 1.8$ Hz, and the spectrum in the case of smoothing (Fig. 24a) remains essentially the same as Fig. 23a. The unsmoothed spectral power (Fig. 24b) reveals some unusual anomalies which at first glance appear to be caused by aliasing (frequency folding). The use of a bandpass filter and sampling at greater than twice the upper frequency of the band should have eliminated the problem of aliasing. The spectrum has such significant power components extending far outside the passband that one is lead to believe that this phenomenon must be due to the Doppler effect.

The object lesson here is that one must be careful in his selection of analysis so as to avoid biasing the data. The method used heretofore was *raw* spectral estimates; this resulted in a complete breakdown in the power spectrum analysis. The more effective method of analysis on Dopplered signals would be autocorrelation on smoothed estimates of power spectra. The crosscorrelation deteriorates rapidly with Doppler effects and hence has very little value (Fig. 24d).

There is no need to dwell at length on the remaining cases, since the same reasoning for the two cases just considered can be applied. It will suffice to say that the smoothed estimates of power spectrum remain relatively unchanged for all the cases of Doppler considered here, and it dramatizes the usefulness of smoothing. The crosscorrelation appears to be very sensitive to Doppler, and a shift of 0.8 Hz has a very damaging effect. Had the signal contained any significant additive noise, the crosscorrelation would have been all but useless for any Doppler shifts of more than 0.8 Hz. The Doppler effect is essentially symmetrical for corresponding values of *up* or *down* Doppler.

We can translate our Doppler shifts given in Table 4 to velocity terms by application of either Eq. 52 or 56. Equation 52 is for a fixed receiver and moving target, and if we assume the values $\mathbf{c} = 5000$ ft/sec (velocity of sound in water), $\mathbf{f} = 200$ Hz, and $\mathbf{f}' = 200.4$ Hz, then $\Delta \mathbf{F} = 0.4$ Hz. The velocity of the source or target for a Doppler shift of 0.4 Hz corresponds to 6.8 mi/hr or 5.9 knots. Since all Doppler shifts were based on increments of 0.4 Hz, we can get the corresponding velocity for any of the cases given in Table 4.

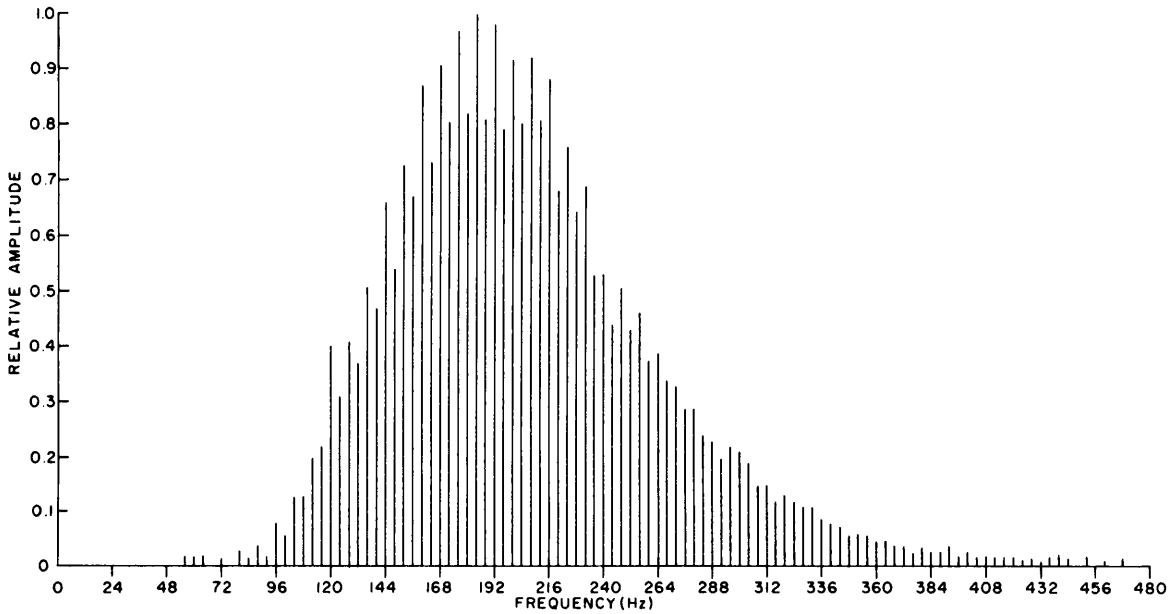

(a) Smoothed spectrum

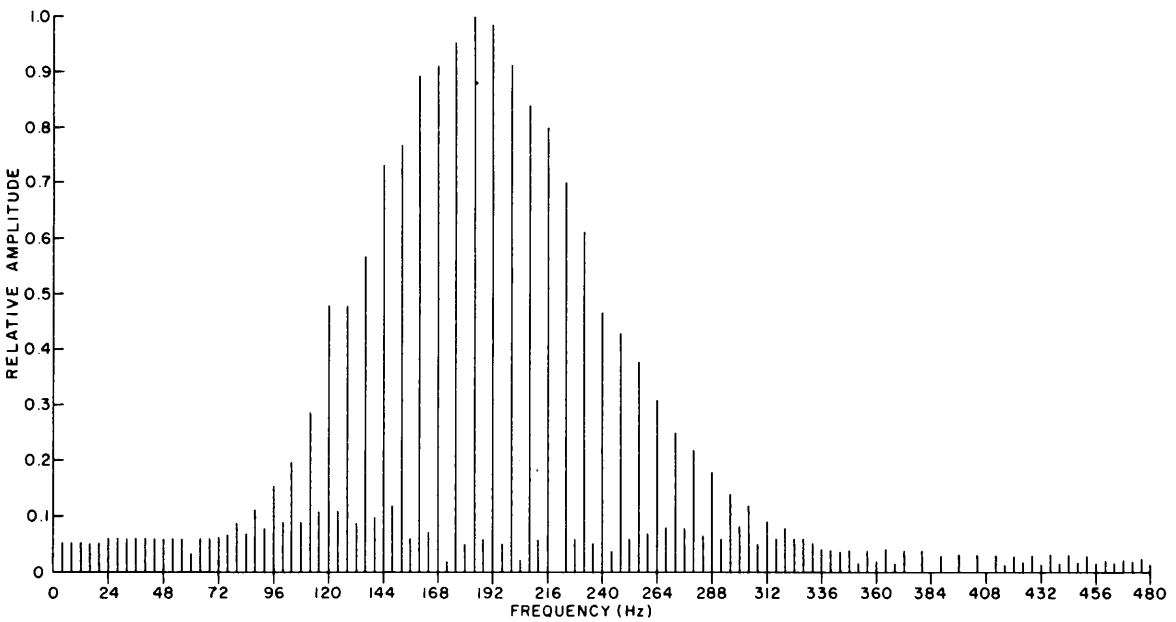

(b) Unsmoothed spectrum

Fig. 23 – Doppler effects on PN power spectrum and correlations (Case 2 of Table 4: BW = 150-250 Hz; Doppler shift = 0.4 Hz)

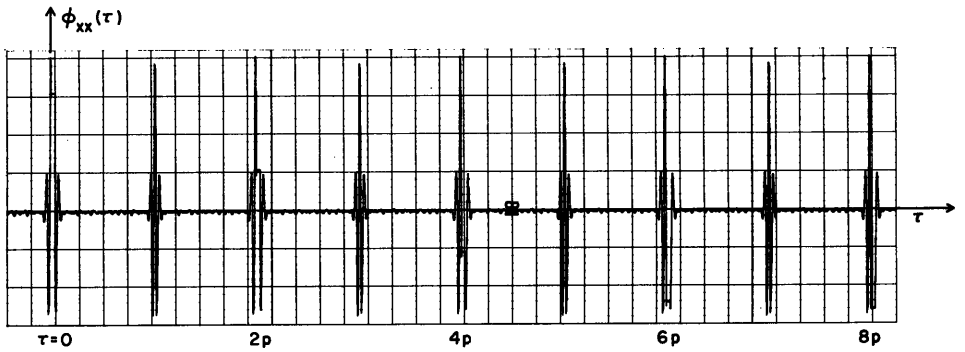

(c) Autocorrelation

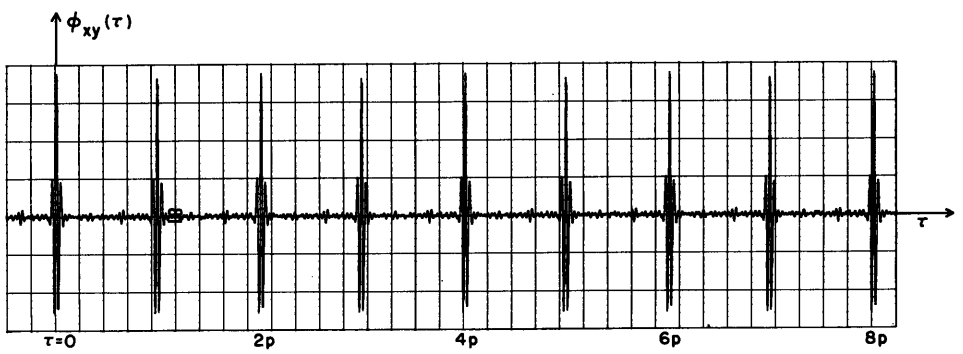

(d) Crosscorrelation of the reference PN against Case 2

Fig. 23 – Doppler effects on PN power spectrum and correlations (Case 2 of Table 4: BW = 150-250 Hz; Doppler shift = 0.4 Hz)–Continued

Equation 56 corresponds to a moving receiver and moving source. If we assume the receiver and source have equal velocities, the resulting velocity for a Doppler shift of 0.4 Hz is 3.4 mi/hr or 2.96 knots. Similarly, as in the previous case, all velocity terms could be found, since all Doppler shifts were multiples of 0.4 Hz. The case of moving receiver and source with equal velocities corresponds to two-way propagation with a fixed receiver.

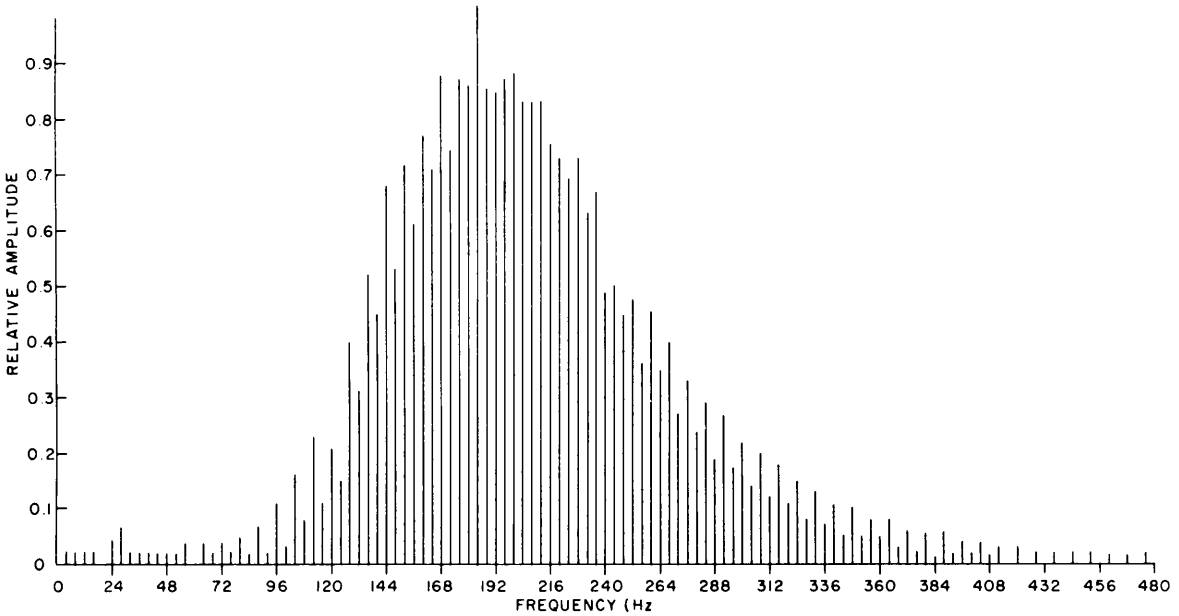

(a) Smoothed spectrum

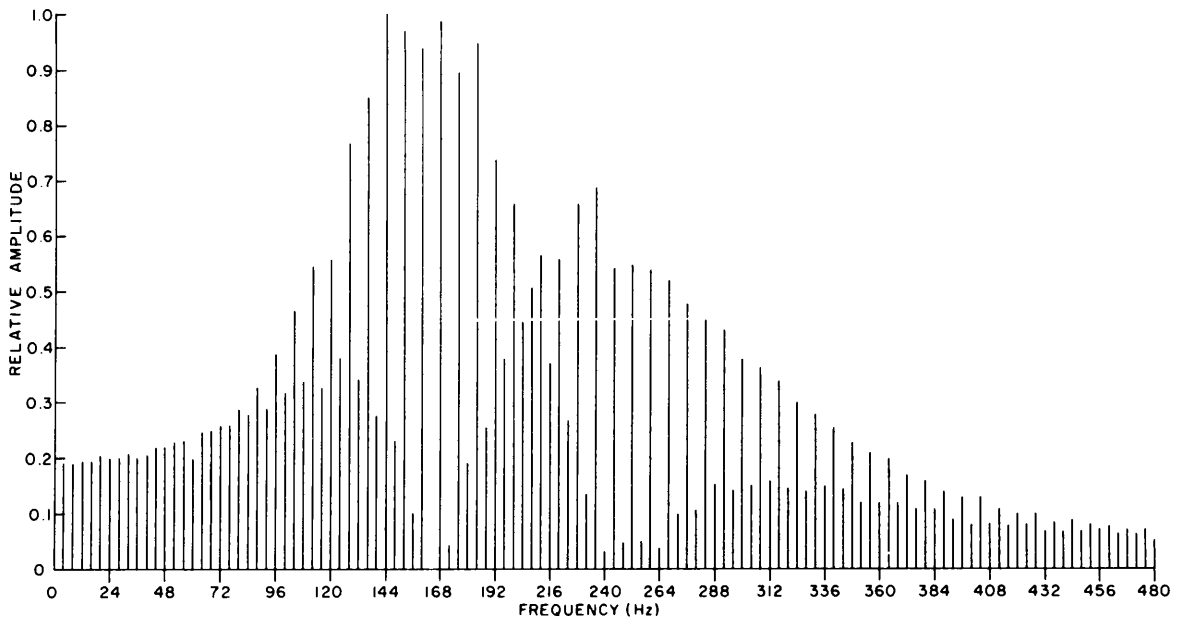

(b) Unsmoothed spectrum

Fig. 24 – Doppler effects on PN power spectrum and correlations (Case 6 of Table 4: BW = 150-250 Hz; Doppler shift = 1.8 Hz)

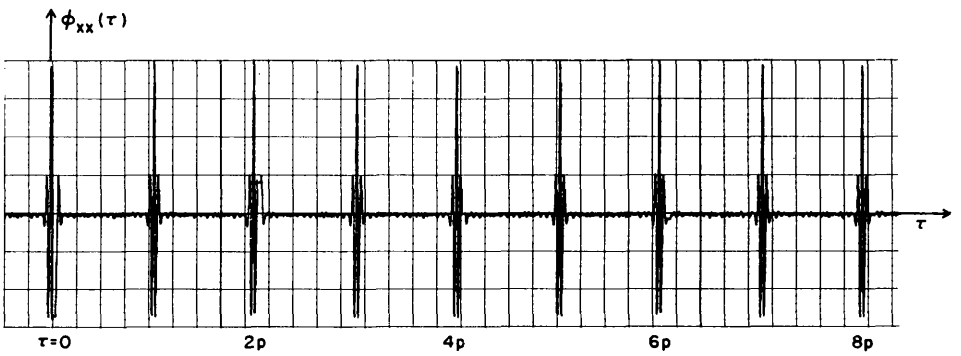

(c) Autocorrelation

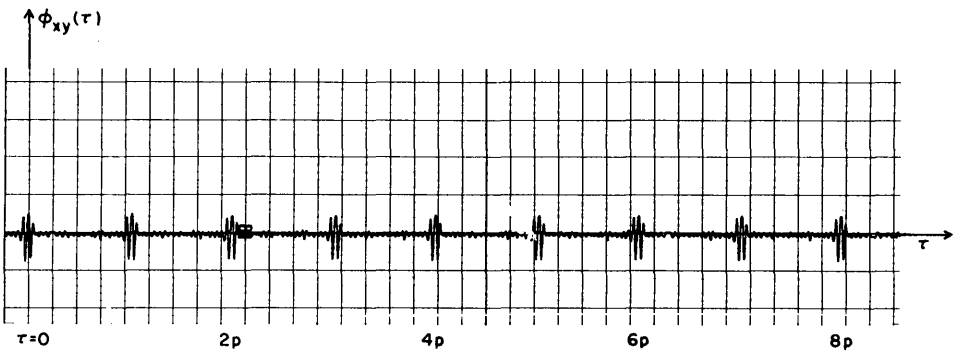

(d) Crosscorrelation of the reference PN against Case 6

Fig. 24 – Doppler effects on PN power spectrum and correlations (Case 6 of Table 4: BW = 150-250 Hz; Doppler shift = 1.8 Hz)–Continued

CONCLUSIONS

Power spectrum estimates of sampled pseudo-random sequences have been presented. The pseudo-random sequences were generated by a linear shift register of length n bits, employing modulo-2 feedback. Only bandlimited maximal length sequences were considered in this analysis. PN sequences were chosen for this study because of their deterministic properties and their desirable autocorrelation functions that are approximately zero outside a narrow peak at zero tau. Both the autocorrelation and crosscorrelation were carried along with the power spectrum analysis for comparison.

The preliminary check of the output power in decibels versus shift rate on maximal length sequences revealed that the output was essentially constant for all maximal sequence lengths. There are a number of points to be noted about the power spectrum of the PN signal. First, it is a line spectrum with frequencies at multiples of the fundamental frequency (shift rate per bit). Second, since the binary waveform is a constant-amplitude square wave and hence has constant power, there is a scale factor inversely proportional to the period of the sequence. This means that if the period of the sequence is doubled, the spectral lines become twice as dense and the power of each line is reduced by a factor of two. Third, there is an envelope of the spectrum that is determined by the digit period of the waveform. This means that the bandwidth is independent of the length of the waveform but is determined solely by the digit period, i.e., how often the waveform switches.

We have studied the power spectrum by limiting the sample size and the period of the PN to the constraints imposed by the computer facilities. Our estimates of spectra were computed on single time functions, although spectral analysis need not be so restricted. We could have calculated cross-spectra from two or more concurrent time functions. Sometimes there is some difficulty in justifying why one prefers the power spectrum over the autocorrelation. Since they are Fourier transforms of each other, it would appear to be purely a matter of convenience as to which one is used in any particular situation. Our studies of power spectrum with the effects of additive noise, multipath, and Doppler tend to favor power spectrum over correlation, particularly in the case of Doppler effects. In the design of optimum filter characteristics for protection of signals against noise in communication systems, the filter designer invariably turns to the power spectrum as the final criterion of adequate design and performance.

Some authors [20] contend that the practice of spectrum analysis is entering either its third or fourth era. Their conclusions are based on the slow computational speed of earlier methods such as the periodogram or mean lagged products for obtaining power spectra. They feel that the approach for computational purposes should be via the fast Fourier transform, and this should greatly reduce computation effort.

Another procedure recommended in spectral analysis techniques that may be useful in special applications is *prewhitening* and *recoloring*. Prewhitening requires advanced knowledge of the spectrum and involves applying a special filter (analog or digital) to the data which will result in the filtered data having a white (flat) spectrum. The filter must have a frequency response that has valleys where the spectrum of the data has peaks and vice versa. A flat spectrum is desired for the filtered data since this assumption is made in the derivation of the uncertainty formulas. A recoloring operation has to take place at the finish of the computations in order to obtain the original spectrum. This involves the application of a filter which is the reverse of the prewhitening filter.

REFERENCES

1. Blackman, R. B., and Tukey, J. W., "The Measurement of Power Spectra," Dover, 1958

2. Golomb, S. W., "Digital Communications with Space Applications," Prentice-Hall, 1964

3. Birdsall, T. G., and Ristenbatt, M. P., "Introduction to Linear Shift-Register Generated Sequences," Technical Report 90, University of Michigan Research Institute, Oct. 1958

4. Gold, R., "Optimal Binary Sequences for Spread Spectrum Multiplexing," Magnavox Research Laboratories, Torrance, California

5. Allen, W. B., and Westerfield, E. C., "Digital Compressed Time Correlators and Matched Filters for Active Sonar," J. Acoust. Soc. Amer 36:121 (Jan. 1964)

6. Bendat, J. S., and Piersol, A. G., "Measurement and Analysis of Random Data," Wiley, 1966

7. Shannon, C. E., "Communication in the Presence of Noise," Proc. I.R.E. 37:10 (Jan. 1949)

8. Winder, A. A., and Loda, C. J., "Introduction to Acoustical Space-Time Information Processing," ONR Report ACR-63, Jan. 1963

9. McCoy, C., Jr., and Peterson, H. L., "A Magnetic Digital Recording System for Field Use," NRL Report 6016, 1963

10. Ralston, A., and Wilf, H. S., "Mathematical Methods for Digital Computer," Wiley, 1962

11. Wainstein, L. A., and Zubakov, V. D., "Extraction of Signals from Noise," Prentice-Hall, 1962

12. Rowe, H. E., "Signals and Noise in Communication Systems," Van Nostrand, 1965

13. Davenport, W. B., and Root, W. L., "An Introduction to the Theory of Random Signals and Noise," McGraw-Hill, 1958

14. Bennett, W. R., and Davey, J. R., "Data Transmission," Wiley, 1960

15. Young, T. Y., "Representation and Analysis of Signals, Part XVI – Representation and Detection of Multiple-Epoch Signals," Carlyle Barton Laboratory, The Johns Hopkins University, May 1963

16. Horton, J. W., "Fundamentals of Sonar," United States Naval Institute, Annapolis, NavShips 92719, 1957

17. Woodward, P. M., "Probability and Information Theory, with Applications to Radar," Pergamon Press, 1964

18. Gill, T. P., "The Doppler Effect," Logos Press and Academic Press, 1965

19. Jenkins, F. A., and White, H. E., "Fundamentals of Optics," McGraw-Hill, 1950

20. Godfrey, M. D., and Tukey, J. W., "Modern Techniques of Power Spectrum Estimation," Princeton University, Institute for Advanced Studies (Vienna) and Bell Telephone Laboratories, 1965

APPENDIX A

PROPERTIES OF PSEUDO-RANDOM SEQUENCES

SHIFT AND ADD PROPERTY

Let the ith digit of a maximum length sequence be designated by x_i; then by the recurrence relationship* we have

$$x_i = x_{i-a} \oplus x_{i-b} \tag{A1a}$$

and

$$x_{i+\tau} = x_{i-a+\tau} \oplus x_{i-b+\tau}, \tag{A1b}$$

where τ is some integral multiple of clock periods.

Adding these equations (module 2), we get

$$x_i \oplus x_{i+\tau} = x_{i-a} \oplus x_{i-b} \oplus x_{i-a+\tau} \oplus x_{i-b+\tau}. \tag{A2}$$

Let $y_i = x_i \oplus x_{i+\tau}$. Then

$$y_{i-a} = x_{i-a} \oplus x_{i+\tau-a} \tag{A3a}$$

and

$$y_{i-b} = x_{i-b} \oplus x_{i+\tau-b} \tag{A3b}$$

Similar to Eq. A1a we have

$$y_i = y_{i-a} \oplus y_{i-b}. \tag{A4}$$

Thus y_i satisfies the same recurrence relationship as x_i.

The subscripts a and b refer to the shift register stages employed in the mod-2 addition. Since both sequences are maximal length, each will contain all possible n-tuples. Hence the two sequences will contain the same n-tuple binary bits. Therefore the sequence generated by the y_i's will be the same as that generated by the x_i's but shifted in time.

*S. W. Golomb, "Digital Communications with Space Applications," Prentice-Hall, 1964; T. G. Birdsall and M. P. Ristenbatt, "Introduction to Linear Shift-Register Generated Sequencies," Technical Report 90, University of Michigan Research Institute, Oct. 1958.

DERIVATION OF THE AUTOCORRELATION FUNCTION

The output sequence associated with the PN generator is a series of 1's and 0's representing the two states of the flip-flops. We would like to make a transition from the *shift and add* property to a *shift and multiply* property. This later property will enable us to solve the integral for the autocorrelation function given by Eq. 4. The property of isomorphic groups given in Table A1, where "1" corresponds to "-1" and "0" to "1," we have the modulo-2 addition with "0" and "1" corresponding to the multiplication of "1" and "-1".

Table A1.
Truth Table for the Isomorphic Groups $\{1, 0; +\}$ and $\{-1, 1; \cdot\}$.

A	B	$A \oplus B$	A	B	$A \cdot B$
1	0	1	-1	1	-1
0	1	1	1	-1	-1
0	0	0	1	1	1
1	1	0	-1	-1	1

Corresponding to Eq. 3, we have the *shift and multiply* property, namely,

$$x(t)\, x(t + \tau_1) = x(t + \tau_2), \tag{A5}$$

where τ_1 and τ_2 are some integral number of clock periods. This *shift and multiply* will allow a solution to the correlation integral as follows:

$$R_x(\tau_1) = \frac{1}{T}\int_0^T x(t)\, x(t + \tau_1)\, dt, \text{ for } \tau \neq 0,$$

$$= \frac{1}{T}\int_0^T x(t + \tau_2)\, dt, \tag{A6}$$

where

$$T = (2^n - 1)\,\Delta t = \frac{2^n - 1}{f_s}.$$

On each subinterval of length Δt, $x(t + \tau_2)$ is either plus or minus one. Letting $a_i = \pm 1$ and rewriting our equation in the form

$$R_x(\tau_1) = \frac{1}{T} \sum_{i=1}^{2^n-1} \int_{(i-1)\Delta t}^{i\Delta t} a_i \, dt = \frac{1}{T} \sum_{i=1}^{2^n-1} a_i \int_{(i-1)\Delta t}^{i\Delta t} dt$$

$$= \frac{1}{T} \sum_{i=1}^{2^n-1} a_i [t]_{(i-1)\Delta t}^{i\Delta t} = \frac{1}{T} \sum_{i=1}^{2^n-1} a_i \Delta t \tag{A7}$$

and substituting

$$T = (2^n - 1)\ \Delta t,$$

we get

$$R_x(\tau_1) = \frac{1}{2^n - 1} \sum_{i=1}^{2^n-1} a_i.$$

Postulate A (balance), written in terms of the "-1" and "1" representation of the group, states that in each period of the sequence the number of minus ones will be exactly one more than the number of plus ones. Hence

$$\sum_{i=1}^{2^n-1} a_i = -1.$$

Therefore for $\tau \neq 0$

$$R_x(\tau_1) = -\frac{1}{2^n - 1} \tag{A8}$$

and for $\tau = 0$

$$R_x(0) = \frac{1}{T} \int_0^T x^2(t)\ dt,$$

and since $x^2(t)$ will always equal $+1$,

$$R_x(0) = \frac{1}{T} \int_0^T dt = 1. \tag{A9}$$

Since the autocorrelation function of a random binary sequence is linear, we can write the correlation function as

$$\mathbf{R_x}(\tau) = \begin{cases} 1 - |\tau| \dfrac{2^n}{2^n - 1}, & \text{for } |\tau| \leq 1 \text{ bit} \\ -\dfrac{1}{2^n - 1}, & \text{for } |\tau| \geq 1 \text{ bit} \end{cases} \tag{A10}$$

APPENDIX B

MATHEMATICAL CONCEPTS

IMPULSE FUNCTION

The Dirac delta function, sometimes called the impulse function or unit area function, is defined by

$$\delta(t) = 0, \qquad \text{for } t \neq 0, \tag{B1a}$$

and

$$\int_{-\infty}^{\infty} \delta(t)\, dt = 1. \tag{B1b}$$

Due to the singular character of the delta function, it has meaning only so long as a subsequent integration over its argument is carried out. Keeping this in mind we can write some basic properties of the delta function:*

$$\begin{aligned} \delta(x) &= \delta(-x); \\ \delta'(x) &= \delta'(-x); \\ x\,\delta(x) &= 0; \\ x\,\delta'(x) &= -\delta(x); \\ \delta(ax) &= a^{-1}\delta(x), \qquad \text{for } a > 0; \\ f(x)\,\delta(x-a) &= f(a)\,\delta(x-a). \end{aligned} \tag{B2}$$

One of the more useful properties of a delta function is its so called *sifting property*, or equivalently, how the delta function acts as an operator on a continuous function. If $x(t)$ is continuous at $t = 0$, then as a consequence of Eqs. B1

$$\int_{-\infty}^{\infty} \delta(t)\, x(t)\, dt = x(0) \tag{B3a}$$

and

*L. I. Schiff, "Quantum Mechanics," McGraw-Hill, Chapter 2, 1949.

$$\int_{-\infty}^{\infty} \delta(t-a)\, x(t)\, dt = x(a). \tag{B3b}$$

This useful property of the delta function will be used in the section *Power Spectrum.*

FOURIER TRANSFORMS

Given f(t) as a complex valued function of a real variable t defined on $-\infty < t < \infty$ we form the integral

$$F(\omega) = \int_{-\infty}^{\infty} f(t)\, e^{-j\omega t}\, dt. \tag{B4}$$

If this integral exists for every real value of the parameter ω, it defines a function $F(\omega)$ known as the Fourier transform of f(t). A sufficient condition for this integral to exist is for f(t) to be absolutely integrable in the sense

$$\int_{-\infty}^{\infty} |f(t)|\, dt < \infty. \tag{B5}$$

The function $F(\omega)$ is in general complex and can be represented as

$$F(\omega) = R(\omega) + j\,X(\omega) = A(\omega)\, e^{j\phi(\omega)}, \tag{B6}$$

where $A(\omega)$ is the magnitude of the Fourier spectrum, $A^2(\omega)$ is the energy spectrum, and $\phi(\omega)$ is the phase of $F(\omega)$.

The inversion formula, permitting the representation of f(t) in terms of its Fourier transform $F(\omega)$ is given by

$$f(t) = \frac{1}{2\pi} \int_{-\infty}^{\infty} F(\omega)\, e^{j\omega t}\, d\omega. \tag{B7}$$

Equations B4 and B7 are called Fourier transform pairs.

A useful identity in frequency analysis is the Parseval relation. For two real-valued functions f(t) and g(t) there exists a time and frequency domain relationship such that

$$\int_{-\infty}^{\infty} f(t)\, g(t)\, dt = \frac{1}{2\pi} \int_{-\infty}^{\infty} F(-\omega)\, G(\omega)\, d\omega = \frac{1}{2\pi} \int_{-\infty}^{\infty} F(\omega)\, G(-\omega)\, d\omega, \tag{B8}$$

and, for complex functions,

$$\int_{-\infty}^{\infty} f(t)\ g^*(t)\ dt = \frac{1}{2\pi} \int_{-\infty}^{\infty} F(\omega)\ G^*(\omega) d\omega, \tag{B9}$$

where $G^*(\omega)$ is the complex conjugate of $G(\omega)$. Notice that if $g(t)$ is real valued, then its transform $G(\omega)$ must satisfy

$$G(\omega) = G^*(-\omega) \tag{B10a}$$

or

$$G^*(\omega) = G(-\omega). \tag{B10b}$$

CONVOLUTION

In signal analysis the convolution theorem is a powerful tool. Given two functions $f_1(x)$ and $f_2(x)$ we form the integral

$$f(x) = \int_{-\infty}^{\infty} f_1(\lambda)\ f_2\ (x - \lambda)\ d\lambda. \tag{B11}$$

This integral defines a function $f(x)$ known as the convolution of $f_1(x)$ and $f_2(x)$, often written as

$$f(x) = f_1(x) * f_2(x). \tag{B12}$$

The convolution theorem states that the Fourier transform of the convolution of two functions is the product of their individual transforms (e.g., the product of two functions in the frequency domain is the convolution of these two functions in the time domain and vice versa).

POWER SPECTRUM

If μ watts represent the amount of power dissipated in a 1-ohm resistance and if the portion of μ arising from the components having frequencies between f and f + df is denoted by $\mathbf{W(f)\ df}$, then

$$\mu = \int_{-\infty}^{\infty} \mathbf{W(f)\ df} = \langle x^2(t) \rangle, \tag{B13}$$

where $\mathbf{W}(f)$ is called the power spectrum or power spectral density of $x(t)$ and has the dimensions of energy. The quantity expressed by Eq. B13 is called average power, or mean-square voltage.

If $x(t)$ is a periodic time function with period T and has a Fourier series representation of

$$x(t) = \frac{1}{T} \sum_{n=-\infty}^{\infty} C_n e^{jn\omega_0 t}, \qquad \omega_0 = \frac{2\pi}{T}, \tag{B14}$$

where

$$C_n = \int_0^T x(t)\, e^{-jn\omega_0 t}\, dt,$$

the power spectrum of $x(t)$ becomes

$$\mathbf{W}(f) = \sum_{n=-\infty}^{\infty} \left|\frac{C_n}{T}\right|^2 \delta(f - nf_0). \tag{B15a}$$

The total mean-square value of $x(t)$ is given by

$$\int_{-\infty}^{\infty} \mathbf{W}(f)\, df = \sum_{n=-\infty}^{\infty} \left|\frac{C_n}{T}\right|^2, \tag{B15b}$$

and by Parsenal's theorem

$$\int_{-\infty}^{\infty} \mathbf{W}(f)\, df = \sum_{n=-\infty}^{\infty} \left|\frac{C_n}{T}\right|^2 = \frac{1}{T} \int_0^T |x(t)|^2\, dt. \tag{B15c}$$

We see from Eq. B15a that the power spectrum consists of a series of impulses at the component frequencies of $x(t)$, where the area of each impulse is the *strength* of power in the frequency component. Thus, for a periodic function the power spectrum is discrete. It is also apparent from Eq. B15a that $\mathbf{W}(f)$ is never complex and, therefore, does not contain phase information. This implies that the spectral density is not a unique function of $x(t)$.

Since x(t) as defined by Eq. B14 is periodic, and complex, its autocorrelation function is given by

$$R_x(\tau) = \frac{1}{T} \int_{-T/2}^{T/2} x(t)\, x^*(t+\tau)\, dt,$$

and by substitution of x(t) from Eq. B14

$$R_x(\tau) = \sum_{n=-\infty}^{\infty} \left|\frac{C_n}{T}\right|^2 e^{-jn\omega_0\tau}. \tag{B16}$$

We would like to investigate the relationship between spectral density and the autocorrelation function of a periodic time function. Taking the Fourier transform of $R_x(\tau)$ we obtain

$$\int_{-\infty}^{\infty} R_x(\tau)\, e^{-j\omega\tau}\, d\tau = \sum_{n=-\infty}^{\infty} \left|\frac{C_n}{T}\right|^2 \int_{-\infty}^{\infty} e^{-j(\omega - n\omega_0)\tau}\, d\tau. \tag{B17}$$

The integral will yield the Dirac delta function; hence

$$\sum_{n=-\infty}^{\infty} \left|\frac{C_n}{T}\right|^2 \int_{-\infty}^{\infty} e^{-j(\omega - n\omega_0)\tau} d\tau = \sum_{n=-\infty}^{\infty} \left|\frac{C_n}{T}\right|^2 \delta(f - nf_0) = W_x(f). \tag{B18}$$

Thus, for a periodic time function the spectral density and the autocorrelation function are a Fourier-transform pair. This relationship between the autocorrelation and spectral density is the Wiener-Khintchine theorem. The theorem states in part that if an arbitrary function is amenable to Fourier analysis, then its autocorrelation function and power spectrum are Fourier transforms of each other. The relationship can be written as

$$R_x(\tau) = \int_{-\infty}^{\infty} W_x(f)\, e^{j2\pi f\tau}\, df \tag{B19a}$$

and

$$W_x(f) = \int_{-\infty}^{\infty} R_x(\tau)\, e^{-j2\pi f\tau}\, d\tau. \tag{B19b}$$

Notice that

$$R_x(0) = \int_{-\infty}^{\infty} W_x(f)\, df = \sum_{n=-\infty}^{\infty} \left|\frac{C_n}{T}\right|^2$$

in full agreement with our previous definitions of spectral density and mean-square value.

DERIVATION OF POWER SPECTRUM FOR MAXIMAL LENGTH SEQUENCES

By application of Eqs. B19 the power spectrum can be computed for our maximal length sequences, and using a procedure similar to Hampton* we get

$$W_x(f) = \int_{-\infty}^{\infty} R_x(\tau)\, e^{-j2\pi f\tau}\, d\tau. \tag{B20}$$

We use the Fourier series representation for $R_x(\tau)$ as defined by Eq. B14,

$$R_x(\tau) = \frac{1}{T} \sum_{n=-\infty}^{\infty} r_n\, e^{j2\pi n f_0 \tau}, \tag{B21}$$

where $2\pi f_0 = \omega_0$, and we obtain

$$W_x(f) = \int_{-\infty}^{\infty} \frac{1}{T} \sum_{n=-\infty}^{\infty} r_n\, e^{j2\pi n f_0 \tau} e^{-j2\pi f\tau}\, d\tau.$$

Changing the order of integration and summation we get

$$W_x(f) = \frac{1}{T} \sum_{n=-\infty}^{\infty} r_n \int_{-\infty}^{\infty} e^{j2\pi(f-nf_0)\tau}\, d\tau = \frac{1}{T} \sum_{n=-\infty}^{\infty} r_n\, \delta(f - nf_0).$$

Substituting for r_n we get

$$W_x(f) = \frac{1}{T} \sum_{n=-\infty}^{\infty} \left[\int_{-T/2}^{T/2} R_x(\tau)\, e^{-j2\pi n f_0 \tau}\, d\tau \right] \delta(f - nf_0).$$

Due to the sifting property of the delta function the integral will have values only for $f = nf_0$; therefore our expression becomes

*R. L. T. Hampton, "A Hybrid Analog-Digital Pseudo-Random Noise Generator," Spring Joint Computer Conference, pp. 287-301, 1964.

$$\mathbf{W}_x(f) = \frac{1}{T} \int_{-T/2}^{T/2} \mathbf{R}_x(\tau)\, e^{-j2\pi f\tau}\, d\tau \sum_{n=-\infty}^{\infty} \delta(f - nf_0). \tag{B22}$$

The integral in Eq. B22 can be evaluated by application of the relationship given in Eq. A10 for the autocorrelation function. The solution becomes

$$\int_{-T/2}^{T/2} \mathbf{R}_x(\tau)\, e^{-j2\pi f\tau}\, d\tau = \int_{-T/2}^{-T/z} -\frac{1}{z} e^{-j2\pi f\tau}\, d\tau + \int_{-T/z}^{0} \left[1 + \tau\frac{(z+1)}{T}\right] e^{-j2\pi f\tau}\, d\tau$$

$$+ \int_{0}^{T/2} \left[1 - \tau\frac{(z+1)}{T}\right] e^{-j2\pi f\tau}\, d\tau$$

$$+ \int_{T/z}^{T/2} -\frac{1}{z} e^{-j2\pi f\tau}\, d\tau.$$

Our four integrals can be further reduced to three, giving

$$-\frac{2}{z} \int_{T/z}^{T/2} \cos 2\pi f\tau\, d\tau + \int_{-T/z}^{T/z} e^{-j2\pi f\tau}\, d\tau - 2\left(\frac{z+1}{T}\right) \int_{0}^{T/z} \tau \cos 2\pi f\tau\, d\tau$$

and giving finally that

$$\int_{-T/2}^{T/2} \mathbf{R}_x(\tau)\, e^{-j2\pi f\tau}\, d\tau = -\frac{T}{z} \left\{\frac{\sin\,[2\pi f(T/2)]}{2\pi f(T/2)}\right\}$$

$$+\frac{T}{z^2}(z+1) \left[\frac{\sin 2\pi f(T/2)\, z}{2\pi f(T/2)\, z}\right]^2, \tag{B23}$$

where $T = z/f_s = 1/f_0$. Substituting in Eq. B22 we get

$$\mathbf{W}_x(f) = \frac{1}{T} \sum_{n=-\infty}^{\infty} \left\{\frac{T}{z^2}(z+1) \left[\frac{\sin 2\pi nf_0(T/2)\, z}{2\pi nf_0(T/2)\, z}\right]^2 - \frac{T}{z} \left[\frac{\sin 2\pi nf_0(T/2)}{2\pi nf_0(T/2)}\right]\right\} \delta(f - nf_0)$$

$$= \sum_{n=-\infty}^{\infty} \left\{\left(\frac{z+1}{z^2}\right) \left[\frac{\sin n(\pi/z)}{n(\pi/z)}\right]^2 - \frac{1}{z} \left(\frac{\sin n\pi}{n\pi}\right)\right\} \delta(f - nf_0)$$

(continued)

$$\mathbf{W}_x(f) = \frac{1}{z^2}\,\delta(f) + \sum_{\substack{n=-\infty \\ n\neq 0}}^{\infty} \frac{z+1}{z^2}\left[\frac{\sin n(\pi/z)}{n(\pi/z)}\right]^2 \delta\left(f - \frac{nf_s}{z}\right), \tag{B24}$$

where f_s = shift rate = zf_0.

APPENDIX C

DEFINITIONS OF STATISTICAL TERMS

There are a few terms associated with the statistical theory of communication that have become an integral part of communication theory. Some of these terms have been tacitly used in the text of this report and deserve further comment. There will be no attempt to prove or develop these terms, since they are given rather comprehensive treatment in present-day literature.* The definitions given here are predicated on an understanding of probability theory, and only a few basic terms associated with probability are included here.

PROBABILITY

If S (for sample space) defines the totality of outcomes in an experiment and A defines the event of interest, then there are three basic definitions associated with probability: relative frequency, the classical definition of probability, and the axiomatic definition of probability.

Relative Frequency

If $n(A)$ = total number of times A has occurred in N trials, then relative frequency of

$$A \triangleq \frac{n(A)}{N} = F_N(A). \tag{C1}$$

The probability of A can be defined as

$$P(A) = \lim_{N \to \infty} \frac{n(A)}{N} = \lim_{N \to \infty} F_N(A).$$

Classical Definition of Probability

Let $N \triangleq$ total number of alternatives and $N(A) \triangleq$ total number of alternatives favorable to A; then the classical definition of probability results:

*L. A. Wainstein and V. D. Zubakov, "Extraction of Signals from Noise," Prentice-Hall, 1962; H. E. Rowe, "Signals and Noise in Communication Systems," Van Nostrand, 1965; W. B. Davenport and W. L. Root, "An Introduction to the Theory of Random Signals and Noise," McGraw-Hill, 1958; W. R. Bennett and J. R. Davey, "Data Transmission," Wiley, 1960; Y. W. Lee, "Statistical Theory of Communication," Wiley, 1960; J. M. Wozencroft and I. M. Jacobs, "Principles of Communication Engineering," Wiley, 1965; A. Papoulis, "Probability, Random Variables, and Stochastic Processes," McGraw-Hill, 1965.

$$\mathbf{P}(\mathbf{A}) = \frac{\mathbf{N}(\mathbf{A})}{\mathbf{N}}. \tag{C2}$$

Axiomatic Definition of Probability

The probability of an event **A** is a number **P**(**A**) assigned to this event such that

$$\mathbf{P}(\mathbf{A}) \geq 0 \text{ (nonnegative)} \tag{C3a}$$

and

$$\mathbf{P}(\mathbf{S}) = 1 \text{ (certain event)}. \tag{C3b}$$

If **A** and **B** are mutually exclusive (disjoint), then

$$\mathbf{P}(\mathbf{A}+\mathbf{B}) = \mathbf{P}(\mathbf{A}) + \mathbf{P}(\mathbf{B}). \tag{C3c}$$

CONDITIONAL PROBABILITY

Given two events **A** and **B**, the conditional probability of **B**, subject to the condition that **A** has occurred, is given by

$$\mathbf{P}(\mathbf{B}/\mathbf{A}) \triangleq \frac{\mathbf{P}(\mathbf{A},\mathbf{B})}{\mathbf{P}(\mathbf{A})}, \qquad \mathbf{P}(\mathbf{A}) \neq 0. \tag{C4a}$$

Also

$$\mathbf{P}(\mathbf{A}/\mathbf{B}) \triangleq \frac{\mathbf{P}(\mathbf{A},\mathbf{B})}{\mathbf{P}(\mathbf{B})}, \qquad \mathbf{P}(\mathbf{B}) \neq 0. \tag{C4b}$$

Note that

$$\mathbf{P}(\mathbf{A},\mathbf{B}) = \mathbf{P}(\mathbf{B}/\mathbf{A})\,\mathbf{P}(\mathbf{A}) = \mathbf{P}(\mathbf{A}/\mathbf{B})\,\mathbf{P}(\mathbf{B}).$$

RANDOM VARIABLES

A random variable is a real-valued function defined over the sample space **S** of a random experiment. The word *random* stresses the fundamental fact that we are dealing with experiments governed by laws of chance rather than any deterministic law. A random variable (r.v.) may be either discrete or continuous.

ENSEMBLE

In a communication system we are not concerned with just a single random time function, but an aggregate of random functions. The infinite aggregate of messages or noise, or of their combination, is called the *ensemble*. When only one function in the ensemble is meant, the function is called a *member function* of the ensemble.

RANDOM PROCESS

A single time history representing a random phenomenon is called a sample function. The collection of all possible sample functions which the random phenomenon might have produced is called a *random process.*

PROBABILITY DENSITY FUNCTION

Any function can be a *probability density function* [denoted $\mathbf{p(x)}$] if it satisfies $p(x) \geq 0$ and

$$\int_{-\infty}^{\infty} p(x)\, dx = 1.$$

ENSEMBLE AVERAGE

Ensemble average is the limit of the arithmetic average or in a communication system it is the limit of a time average. If $\mathbf{x}$ is a discrete r.v.,

$$E\{X\} = \overline{X} = \sum_{i=1}^{n} x_i\, p(x_i), \tag{C5}$$

and if $\mathbf{X}$ is a continuous r.v.

$$E\{X\} = \overline{X} = \int_{-\infty}^{\infty} x\, p(x)\, dx, \tag{C6}$$

where $p(x)$ is the density function.

The ensemble average, statistical average, expected value, and mathematical average are all the same.

MOMENTS

The $\mathbf{n}$th moment for a discrete r.v. $\mathbf{X}$ is

$$E\{X^n\} = \overline{X^n} = \Sigma\, X_i^n\, p(X_i) \tag{C7}$$

and the $\mathbf{n}$th moment for a continuous r.v. $\mathbf{X}$ is

$$E\{X^n\} = \overline{X^n} = \int_{-\infty}^{\infty} X^n\, p(x)\, dx. \tag{C8}$$

STATIONARITY

A random process is said to be *wide-sense stationary* (weakly stationary) when

$$E\{X(t)\} = \text{const.} \tag{C9a}$$

$$E\{X(t_i)X(t_i + \tau)\} = \Phi_{yy}(\tau) = \text{function of } \tau \text{ only, for all i.} \tag{C9b}$$

STATISTICAL INDEPENDENCE

If the joint probability of event **A** and **B** is such that

$$P(A, B) = P(A)\,P(B) \tag{C10a}$$

or if

$$P(A/B) = P(A) \tag{C10b}$$

or if the joint probability density function of **A** and **B** is such that

$$p(A, B) = p(A)\,p(B), \tag{C11}$$

then **A** and **B** are said to be statistically independent.

ERGODICITY

For a process to be ergodic, these requirements must be met

$$E\{X(t_i)\} = \langle X \rangle \qquad \text{for every i} \tag{C12}$$

where < > represents a time average and

$$\langle X \rangle = \lim_{T \to \infty} \frac{1}{2T} \int_{-T}^{T} X(t)\,dt \tag{C13}$$

and $\langle X \rangle$ is a r.v. indicative of the average value of all occurring r.v.'s in the ensemble.

Equation C12 defines first-order ergodicity; similarly the ergodicity of the second order implies

$$E\{X(t_i)X(t_i + \tau)\} = \langle X(t)X(t + \tau) \rangle, \qquad \text{for all i.} \tag{C14}$$

We can further state that ergodicity guarantees stationarity, but the converse is not true.

UNCLASSIFIED
Security Classification

DOCUMENT CONTROL DATA - R & D

(Security classification of title, body of abstract and indexing annotation must be entered when the overall report is classified)

1. ORIGINATING ACTIVITY *(Corporate author)* Naval Research Laboratory Washington, D. C. 20390	2a. REPORT SECURITY CLASSIFICATION Unclassified 2b. GROUP

3. REPORT TITLE

POWER SPECTRUM ESTIMATES OF SAMPLED PSEUDO-RANDOM SEQUENCES

4. DESCRIPTIVE NOTES *(Type of report and inclusive dates)*
An interim report on a continuing problem

5. AUTHOR(S) *(First name, middle initial, last name)*

Caldwell McCoy, Jr.

6. REPORT DATE December 29, 1967	7a. TOTAL NO. OF PAGES 90	7b. NO. OF REFS 20
8a. CONTRACT OR GRANT NO. NRL Problem S01-06 b. PROJECT NO. RF-101-03-44-4054 c. d.	9a. ORIGINATOR'S REPORT NUMBER(S) NRL Report 6673 9b. OTHER REPORT NO(S) *(Any other numbers that may be assigned this report)*	

10. DISTRIBUTION STATEMENT

This document has been approved for public release and sale; its distribution is unlimited

11. SUPPLEMENTARY NOTES	12. SPONSORING MILITARY ACTIVITY Department of the Navy (Office of Naval Research), Washington, D.C. 20360

13. ABSTRACT

This report concerns power spectrum estimates of sampled pseudo-random signals, and shows that for these signals the spectral power is more relevant than, say, the autocorrelation function. The power spectrum estimates considered here assume stationarity and zero means.

The signal under investigation is a pseudo-random noise signal obtained from maximal length sequences. Pseudo-random signals are popular because (a) they can be fashioned with relative ease from linear shift registers, (b) their deterministic waveforms have uniform power throughout their bandwidths, and (c) their autocorrelations are approximately zero outside a narrow peak at zero tau.

This study is concerned with some applied methods and results of these applications to bandlimited signals that have been corrupted by additive-noise, multiple-path, and Doppler effects and that have been processed digitally to obtain correlations and power spectra. The object was to observe the effects on the power spectrum estimates due to these perturbations. The analysis was performed exclusively on filtered maximal length pseudo-random sequences. These filtered sequences were tailored to a bandwidth and sample size to yield optimal results for a given computer memory capability.

DD FORM 1 NOV 65 1473 (PAGE 1)
S/N 0101-807-6801

UNCLASSIFIED
Security Classification

14 KEY WORDS	LINK A ROLE	LINK A WT	LINK B ROLE	LINK B WT	LINK C ROLE	LINK C WT
Communication theory						
Pseudo-random sequences						
Theory						
Power spectra						
Correlation						
Crosscorrelation						
Autocorrelation						
Sampling analysis						
Statistical analysis						
Digital computer analysis						
Filters						